Apoptosis (2025) 30:1482–1501
https://doi.org/10.1007/s10495-025-02112-1

Metabolism-related ALDH1B1 acts as potential predictor and therapeutic target for primary gastrointestinal diffuse large B-cell lymphoma

Qiqi Qiao[1] · Bingyu Liu[2] · Juanjuan Shang[2] · Wenyue Sun[2] · Xiaoli Zhou[1] · Xiaosheng Fang[1,2] · Shunfeng Hu[1,2] · Xin Wang[1,2,3]

Accepted: 28 March 2025 / Published online: 11 April 2025

Abstract

Primary gastrointestinal diffuse large B-cell lymphoma (PGI-DLBCL) is the most common extra-nodal DLBCL. Metabolism-related factors have been associated with tumor progression, but the relationship between abnormal metabolism and prognosis of PGI-DLBCL remains unelucidated. In our study, consensus clustering based on metabolism-related genes classified PGI-DLBCL patients into two metabolic subtypes, and poor prognosis was associated with immunosuppressive microenvironment. A prognostic signature based on five metabolism-related genes (APOE, ALDH6 A1, PLOD2, IKBKB and ALDH1B1) was developed. Patients in high-risk group had a worse prognosis, with an immunosuppressive microenvironment. Moreover, 159 PGI-DLBCL patients were enrolled and divided into training cohort (n = 87) and validation cohort (n = 72). Univariate and multivariate Cox regression analysis showed metabolism-related factors were independent prognostic factors in PGI-DLBCL. A novel model (A-IPI score) combining APOA and NCCN-IPI was developed, and A-IPI score was better than NCCN-IPI score in predicting the prognosis of PGI-DLBCL patients. Furthermore, immunohistochemistry showed that ALDH1B1 was highly expressed in PGI-DLBCL and patients with high ALDH1B1 expression displayed worse prognosis. Moreover, cell proliferation assay revealed that the treatment with IGUANA-1, ALDH1B1 inhibitor, suppressed cell proliferation in DLBCL and IGUANA-1 exerted synergistic anti-tumor effects with PI3K inhibitor duvelisib. Additionally, we found that immune scores, ESTIMATE scores, and stromal scores were higher and the immune checkpoints (CTLA-4, PD-1, PD-L1) were down-regulated in patients with high ALDH1B1 expression. Collectively, our study constructed a novel metabolism-related prognostic model and highlighted the potential of metabolism-related gene ALDH1B1 as prognostic biomarker and drug target in PGI-DLBCL, providing new insights for the development of precision therapies in PGI-DLBCL patients.

Keywords Primary gastrointestinal diffuse large B-cell lymphoma · Metabolism · A-IPI score · Prognostic model · ALDH1B1

✉ Xiaosheng Fang
fxsh_1010@126.com

✉ Shunfeng Hu
HuShunFeng0409@163.com

✉ Xin Wang
xinw007@126.com

[1] Department of Hematology, Shandong Provincial Hospital Affiliated to Shandong First Medical University, No.324, Jingwu Road, Jinan 250021, Shandong, China

[2] Department of Hematology, Shandong Provincial Hospital, Shandong University, No.324, Jingwu Road, Shandong 250021 Jinan, China

[3] Taishan Scholars Program of Shandong Province, Jinan 250021, Shandong, China

Abbreviations

AAMRGs	Amino acid metabolism-related genes
AGR	Albumin to globulin ratio
Alb	Albumin
ALDH	Acetaldehyde dehydrogenase
ALDH1B1	Acetaldehyde dehydrogenase 1B1
APOA	Apolipoprotein A
APOB	Apolipoprotein B
APOABR	Apolipoprotein A to apolipoprotein B ratio
CCK-8	Cell Counting Kit-8
CRGs	Carbohydrate metabolism-related genes
CRP	C-reactive protein

CTRP	Cancer Therapeutics Response Portal
DCA	Decision curve analysis
DEGs	Differentially expressed genes
DLBCL	Diffuse large B-cell lymphoma
EDTA	Ethylenediamine tetraacetic acid
FA	Fatty acid
GA	Glycated albumin
GDSC	Genomics of Drug Sensitivity in Cancer
GLO	Globulin
GLU	Glucose
GO	Gene Ontology
GSEA	Gene Set Enrichment Analysis
Hb	Hemoglobin
HDL-C	High-density lipoprotein cholesterol
HR	Hazard ratio
IDO	Indoleamine 2,3-dioxyge-nase
IHC	Immunohistochemistry
KEGG	Kyoto Encyclopedia of Genes and Genomes
LASSO	Least Absolute Shrinkage and Selection Operator
LDH	Lactate dehydrogenase
LDL-C	Low-density lipoprotein cholesterol
LMRGs	Lipid metabolism-related genes
LPa	Lipoprotein a
MRGs	Metabolism-related genes
NCCN-IPI	National Comprehensive Cancer Network International Prognostic Index
NUSAP1	Nucleolar and spindle associated protein 1
OS	Overall survival
PA	Prealbumin
PFS	Progression-free survival
PGI-DLBCL	Primary gastrointestinal diffuse large B-cell lymphoma
PLT	Platelets
ROC	Receiver operating characteristic
SE	Standard error
TG	Triglycerides

Introduction

Diffuse large B-cell lymphoma (DLBCL) is the most common histologic subtype of lymphoma, as well as a highly heterogeneous and aggressive disease that seriously jeopardizes patients' health and lives [1]. Primary gastrointestinal diffuse large B-cell lymphoma (PGI-DLBCL) is the most common extra-nodal lymphoma, accounting for 40–50% of gastrointestinal lymphomas [2, 3]. PGI-DLBCL originates from the lymphoid tissue of the submucosal layer of the gastrointestinal track, and the most commonly involved site is the stomach, followed by the small intestine and the ileum [4]. The clinical manifestations of most patients in the early stage of disease are mostly similar to other diseases of the digestive system, and it may be difficult to differentiate from other gastrointestinal malignant tumors only imaging or endoscopic diagnosis, which makes early diagnosis difficult and easy to misdiagnose [5].

Due to the special anatomical structure of the gastrointestinal tract, PGI-DLBCL is prone to complications such as gastrointestinal obstruction, perforation, bleeding, and so on, which seriously affects the life quality of patients, and even endangers their lives [6]. Therefore, there is an urgent need for early risk and prognostic assessment of patients with PGI-DLBCL, and then early intervention to improve their prognosis. Currently, the National Comprehensive Cancer Network International Prognostic Index (NCCN-IPI) score is widely used for DLBCL in the rituximab-based era and demonstrates a favorable stratification [7]. However, it is less effective for risk stratification of PGI-DLBCL, and some patients with low NCCN-IPI scores exhibit poor prognosis. In addition, previous study showed that staged-modified IPI was a good predictor for patients with primary gastric DLBCL (PG-DLBCL) [8], but it was mainly based on clinical parameters (such as age, stage, LDH level and so on), and did not adequately take into account molecular biological features, tumor microenvironment and other factors. Besides, PG-DLBCL is highly heterogeneous, and the existing scoring system cannot fully reflect individualized differences [9]. Additionally, gastrointestinal dyspepsia and serious complications may occur in PGI-DLBCL patients undergoing radiotherapy, which may have an impact on the nutritional status and quality of life of the patients [10]. Although the overall survival of PGI-DLBCL treated with chemotherapy has improved, some patients still experience relapse or develop resistance to treatment, resulting in a continued increase in the recurrence, morbidity, and mortality rates of PGI-DLBCL [11].Therefore, there is an urgent need to develop new and accurate risk stratification systems for PGI-DLBCL.

The gastrointestinal tract is the site of direct absorption of various nutrients, such as glucose, amino acids, fatty acids. Thus, PGI-DLBCL may alter the structure and function of the gut, thereby affecting the energy supply and metabolic status of the body [12]. Metabolism-related indicators are important prognostic factors for several cancers such as small intestine cancers, colorectal, and pancreatic cancer [13–15]. Additionally, previous study on cholangiocarcinoma found that HBV infection altered metabolic pathways in hepatocytes, leading to abnormalities in glycogen and lipid metabolism, which might promote tumorigenesis and progression [16]. Reprogramming of glucose metabolism is manifested as an increase in aerobic glycolysis [17], which has been closely related to the activation of proto-oncogenes

like MYC and the inactivation of tumor suppressor genes such as p53 [18, 19]. In DLBCL cells, Akt promoted GLUT1 localization at the plasma membrane through the activation of NF-κ B-dependent transcription, leading to an increase in its glycolytic flux [20], which promoted DLBCL proliferation, suggesting that NF-κB signaling had a potential role in regulating glucose metabolism to stimulate tumor cell survival and proliferation. Furthermore, enhanced glycolysis and lipid biosynthesis in non-Hodgkin's lymphoma might be associated with aberrant activation of the PI3K/AKT/mTOR signaling pathway, which promoted lymphoma cell growth, proliferation and migration [21, 22]. However, the relationship between abnormal metabolism and the prognosis of PGI-DLBCL and its mechanisms need to be further explored.

In this study, we used multiple bioinformatics methods to explore the prognostic role and regulatory mechanisms of metabolism-related genes in DLBCL, constructed prognostic features and clustered subtypes based on metabolism-related genes, and investigated the relationships between metabolism-related genes and the immune microenvironment. In addition, since metabolism-related indicators have been found to be strongly associated with multiple gastrointestinal solid tumors, we investigated the prognostic significance of metabolism-related factors in patients with PGI-DLBCL and comprehensively analyzed clinicopathological features of patients to establish a prognostic model for PGI-DLBCL. The predictive performance of the new model was validated in multiple dimensions, and its superiority was revealed by comparing it with existing prognostic scoring systems. More importantly, the high expression of acetaldehyde dehydrogenase 1B1 (ALDH1B1), a metabolism-related molecule, was associated with worse prognosis in PGI-DLBCL, and targeting ALDH1B1 inhibited cell growth and showed synergistic anti-tumor effects with PI3K inhibitor duvelisib.

Materials and methods

Patients and cell lines

We recruited PGI-DLBCL patients according to the criteria defined by Lewin et al. [23, 24]. Only those patients presenting with gastrointestinal symptoms (such as abdominal pain, ulcerative symptoms, intestinal obstruction, and intestinal hemorrhage) were included in this study [23, 24]. Our study included 159 PGI-DLBCL patients (102 patients with gastric DLBCL and 57 patients with intestinal DLBCL) who were newly diagnosed in Shandong Provincial Hospital from January 2010 to February 2024. Patients were randomly divided into training cohort ($n = 87$) and validation cohort ($n = 72$) based on "randomizr" R package. Pathologic specimens were obtained by endoscopic biopsy and surgical resection, re-examined by experienced histopathologists, and the diagnosis was confirmed according to the WHO hematological malignant tumor classification system. The following patients were included in the study: (1) pathologically diagnosed with gastrointestinal DLBCL, (2) no prior chemotherapy, radiotherapy, surgery, or immunotherapy, (3) no prior history of malignancy or immunosuppression, and (4) with complete clinical information and follow-up data. Exclusion criteria were (1) prior history of malignancy, (2) prior chemotherapy, radiotherapy, surgery, or immunotherapy3], (3) incomplete clinical and follow-up data, and (4) death from other causes. Two cohorts followed the same inclusion and exclusion criteria. Progression-free survival (PFS) referred to the time from diagnosis to disease recurrence or disease progression. Overall survival (OS) was measured from the date of diagnosis to the date of death from any cause or last follow-up. The study was conducted in accordance with the Declaration of Helsinki. The study was approved by the Research Ethics Committee in Shandong Provincial Hospital. OCI-LY1 (RRID: CVCL_1879) and OCI-LY3 (RRID: CVCL_8800) cells were purchased from ATCC, cultured in IMDM (Gibco, CA, USA) supplemented with 10% fetal bovine serum (HyClone, UT, USA), 1% penicillin/streptomycin mixture, and 2 mM glutamine, and incubated at 37 °C in humidified air containing 5% CO2. All human cell lines were examined for short tandem repeat (STR) and mycoplasma infection periodically.

Data sources

We systematically explored publicly available datasets and corresponding clinical information of DLBCL and PGI-DLBCL patients from the GEO database (https://www.ncbi.nlm.nih.gov/geo/). In our study, five datasets were included, GSE23647 (DLBCL, $n = 19$; control, $n = 42$), GSE32018 (DLBCL, $n = 22$; control, $n = 13$), GSE181063 (DLBCL, $n = 1037$), GSE10846 (DLBCL, $n = 514$) and GSE66770 (PGI-DLBCL, $n = 15$; non-PGI-DLBCL, $n = 57$, non-PGI-DLBCL referred to lymph node tissue from DLBCL). We obtained 355 carbohydrate metabolism-related genes, 471 lipid metabolism-related genes, and 358 amino acid metabolism-related genes from the Kyoto Encyclopedia of Genes and Genomes (KEGG) pathway database (https://www.genome.jp/kegg/pathway.html#global), the Molecular Charact erization Database (MsigDB, v7.5.1, https://www.gsea-msigdb.org/) and previous studies works [25–27], and a total of 1049 metabolism-related genes (MRGs) were eventually obtained.

In silico analyses

The "limma" R package of the R software was applied to analyze the differential expression of mRNAs ($P < 0.05$). The "ConsensusClusterPlus" R package categorized patients into subgroups with different expression patterns. Least Absolute Shrinkage and Selection Operator (LASSO) regression was used to construct the metabolism-related genes prognostic signature. Furthermore, we utilized the "clusterProfiler" package for Gene Ontology (GO) enrichment analysis, KEGG pathways analysis, and Gene Set Enrichment Analysis (GSEA) of genes. The criteria for pathways considered to be remarkably enriched were as follows: P value < 0.05, and false discovery rate (FDR) q value < 0.05. The "CIBERSORT" R package was applied to analyze the samples for immune infiltration. The box plot was implemented by the R software package ggplot2 and the heatmap was displayed by the R software package heatmap. Based on Cancer Therapeutics Response Portal (CTRP) (https://portals.broadinstitute.org/ctrp/) and Genomics of Drug Sensitivity in Cancer (GDSC) database (https://www.cancerrxgene.org/), oncoPredict was used to assess differences in drug sensitivity in patients of different groups with ALDH1B1 expression.

Cell proliferation assay

Cell proliferation was assessed using the Cell Counting Kit-8 (CCK-8) assay kit (CK04, DOJINDO, Japan) and Multiskan GO Microplate Reader (Thermo Scientific, IL, USA). IGUANA-1 (HY-148466) was purchased from MedChemExpress.

Immunohistochemistry (IHC)

Antigen retrieval was performed using ethylenediamine tetraacetic acid (EDTA) under high pressure. Slides were then incubated at 37 °C in 3% hydrogen peroxide for 30 min, followed by incubation with goat serum for 30 min to block nonspecific binding. The slides were then incubated with primary antibody overnight at 4 °C. DAB with hematoxylin staining was applied after incubation with biotin-labeled secondary antibody and SABC, respectively, for 30 min at 37 °C on the following day. IHC staining was assessed by two independent observers, who were unaware of group assignment during the experiment. IHC score was calculated by the accumulation of multiplying proportion score (0, <5%; 1, 5–25%; 2, 26–50%; 3, 51–75%; and 4, 76–100%) and intensity score (0, negative; 1, weak; 2, moderate; and 3, strong). Scores of 0–3 were defined as negative expression and 4–12 as positive expression. Primary antibody was ALDH1B1 (15560-1-AP, Proteintech Group).

Statistical analyses

IBM SPSS software version 26 and R software version 4.3.1 were used to analyze the data. Data were tested for homogeneity of variances and normality. Quantitative variables were analyzed using Student's t-test and non-parametric tests. Survival analysis of patients was realized by Kaplan-Meier method and log-rank test using the "survival" R package. Independent prognostic factors were determined by univariate Cox regression analysis and multivariate Cox regression analysis, which were assigned values based on regression coefficients (B). Forest plots were constructed using R package for univariate and multivariate analysis. The optimal cutoff value for new model was determined based on the maximum correlation J statistic (Youden's index) of the receiver operating characteristic (ROC) curves. Time-dependent ROC curve analysis and decision curve analysis (DCA) were conducted to determine the optimal model. Statistical significance was defined as $p < 0.05$ for all statistical tests (*$p < 0.05$, **$p < 0.01$, ***$p < 0.001$).

Results

Metabolism-related genes were closely associated with the survival and immune microenvironment of DLBCL

The flow chart (**Supplemental Fig.** 1) illustrated the process of research, including the exploration of potential molecular mechanisms and the construction and evaluation of new models. Firstly, we downloaded the DLBCL mRNA expression data of GSE23647 and GSE32018 datasets from the GEO database and homogenized the data. 3756 differentially expressed genes (DEGs) were obtained in 41 DLBCL versus 36 reactive hyperplastic tissues (**Supplemental Fig.**2 A). In addition, 1049 metabolism-related genes were collected, and 90 differentially expressed metabolism-related genes in DLBCL were finally identified. Based on univariate survival analysis, 5448 prognosis-related genes in DLBCL were obtained in GSE181063. Moreover, analysis of mRNA expression data in the GSE66770 dataset yielded 3579 DEGs in PGI-DLBCL versus non-PGI-DLBCL (**Supplemental Fig.** 2B-C). Based on the above results, 14 differentially expressed metabolism-related prognostic genes were finally obtained (Fig. 1A, **Supplemental Table**1).

Based on the expression of 14 metabolism-related prognostic genes, we clustered the 1037 patients in the GSE181063 dataset into different metabolism-related

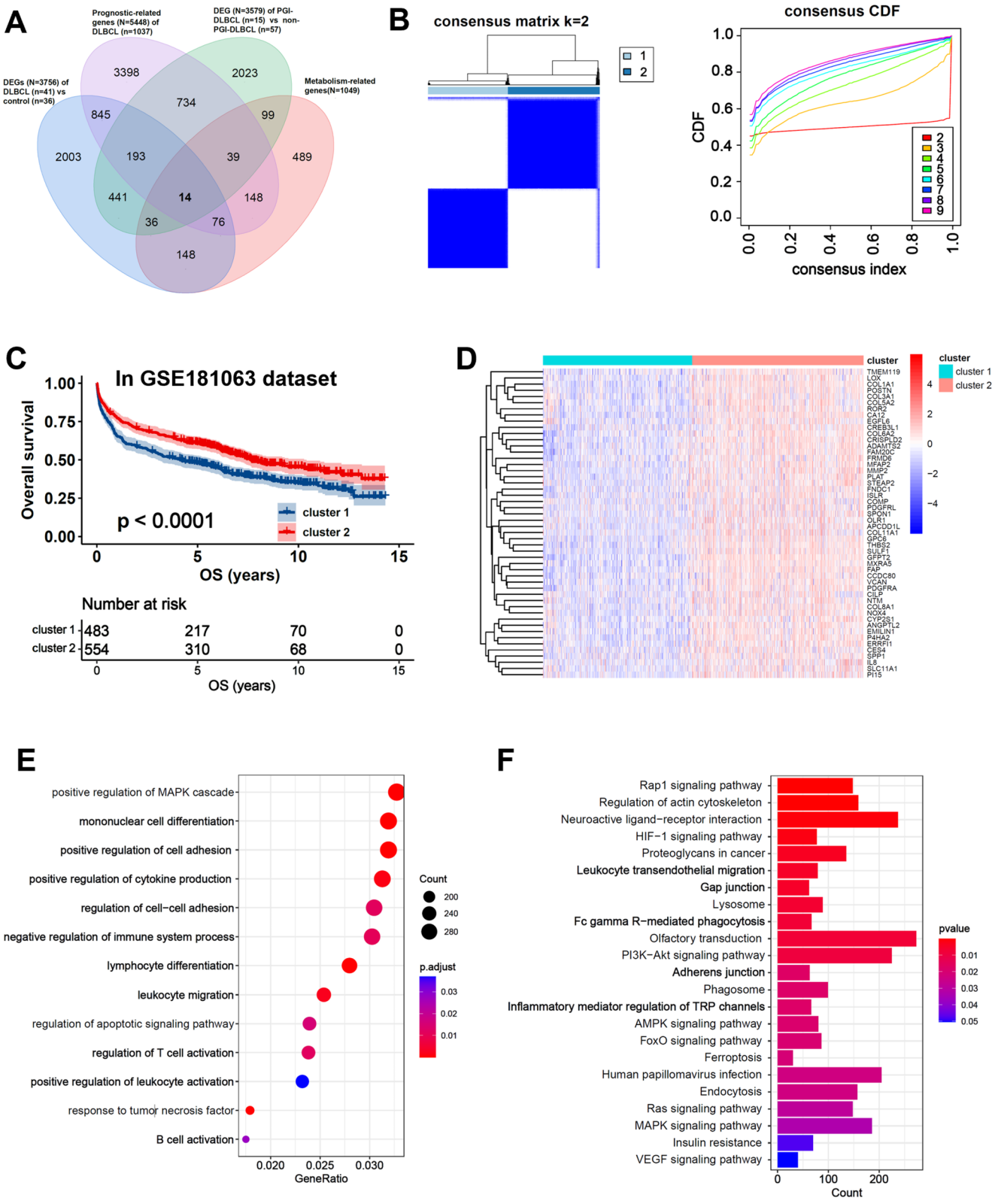

molecular subgroups by consensus clustering. By increasing the clustering variable (k) from 2 to 9, we found that consensus clustering was most appropriate when k = 2 (Fig. 1B, **Supplemental Fig.**3 A). Survival analysis showed that there was a difference in OS between the two groups, with patients in cluster 1 having a significantly worse prognosis

Fig. 1 Metabolism-related genes were associated with the survival of DLBCL. (A) Venn plot showed 14 differentially expressed metabolism-related prognostic genes in PGI-DLBCL. DEGs between DLBCL and control were obtained from GSE23647 (DLBCL, $n = 19$; control, $n = 42$) and GSE32018 (DLBCL, $n = 22$; control, $n = 13$) datasets. Prognostic-related genes were obtained from GSE181063 (DLBCL, $n = 1037$) dataset. DEGs between PGI-DLBCL and non-PGI-DLBCL were obtained from GSE66770 (PGI-DLBCL, $n = 15$; non-PGI-DLBCL, $n = 57$) dataset. (B) Consensus matrix heatmap based on metabolism-related genes found that the optimal value for consensus clustering was K = 2. (C) Survival curve showed the significant difference of OS between the two clusters. (D) Heatmap of the top 50 differentially expressed genes between the two clusters. (E) Bubble plot of GO enrichment of differentially expressed genes between the two clusters. Larger bubbles indicated more enriched genes, and darker red color indicated more pronounced differences. (F) Enrichment of biological functions of differential genes between two clusters by KEGG enrichment analysis. Deeper red depth indicated more obvious differences, and longer bars indicated more enriched genes

than those in cluster 2 ($P < 0.0001$) (Fig. 1C). The top 50 DEGs were selected for heatmap visualization, and significant differences in gene expression were found between the two groups of patients (Fig. 1D). Subsequently, we performed GO and KEGG analysis of the DEGs between cluster 1 and cluster 2. The results showed that the DEGs between both clusters were significantly enriched in the biological processes of inflammatory response, immune response and cell adhesion ($P < 0.05$, FDR < 0.05) (Fig. 1E-F). The above results indicated that immune regulation might play a crucial role in the survival of both clusters of patients.

In addition, differences in immune cell infiltration between the two clusters were assessed using the CIBERSORT algorithm. Cluster 1 had a higher level of infiltration of B cells, T cells and plasma cells, whereas cluster 2 was dominated by infiltration of NK cells, macrophages, mast cells, and neutrophils (Fig. 2A). The correlation of infiltration between immune cells is demonstrated in **Supplemental Fig.**3B. Furthermore, there were significant differences in immune scores, stromal scores, and ESTIMATE scores between the two clusters of patients ($P < 0.001$) (Fig. 2B-D). We also found that there were significant differences in the expression of immune checkpoints such as CTLA-4, PD-L1 and LAG-3 between the two clusters, and there was a higher expression of immune checkpoints in cluster 2 (Fig. 2E-G), which also implied that there was a better effect of immunotherapy in cluster 2. Taken together, these results suggested that the expression of metabolism-related genes were closely associated with the survival of DLBCL, and the potential mechanism might act by altering the tumor microenvironment and immune cell function.

Construction of metabolism-related genes prognostic signature

Among 14 metabolism-related prognostic genes, 12 genes were selected by LASSO regression, and finally 5 genes were identified by multivariate Cox regression analysis ($P < 0.01$, FDR < 0.05) (Fig. 3A-C). A metabolism-related genes prognostic signature was constructed based on the risk coefficients from the multivariate Cox regression analysis, and the risk score for each patient was calculated according to the following formula: Risk score $= APOA \times (-0.18016) + ALDH6A1 \times 0.278961 + PLOD2 \times (-0.1356) + IKBKB \times (-0.24923) + ALDH1B1 \times 0.225072$ (**Supplemental Table** 2). Patients were divided into high-risk and low-risk groups based on the median risk score, and the box plot showed that the survival of the high-risk group was significantly shorter than that of the low-risk group ($P < 0.0001$) (Fig. 3D, **Supplemental Fig.** 3 C). The Kaplan-Meier curve showed that patients in the high-risk group had significantly worse OS than those in the low-risk group (Fig. 3E). In addition, the risk score was also predictive in GSE10846 dataset, as demonstrated by a worse OS in the high-risk group than in the low-risk group (Fig. 3F).

The heatmap showed the differential gene expression of patients in the high- and low-risk groups (Fig. 4A). In addition, we found that the differentially expressed genes were mainly enriched in the biological processes of DNA replication by GSEA analysis (Fig. 4B), suggesting a difference in cell proliferation between the two risk groups. Furthermore, we tried to analyze the immune cell infiltration in the two risk groups, and found that there was higher infiltration of B cells, plasma cells, monocytes, activated mast cells, and less infiltration of T cells, NK cells, macrophages, and dormant mast cells in the high-risk group (Fig. 4C). Moreover, immune scores, ESTIMATE scores, and stromal scores were lower in the high-risk group than in the low-risk group (Fig. 4D-F). Furthermore, the immune checkpoints such as CTLA-4, PD-1, PD-L1 were down-regulated in the high-risk group than in the low-risk group (Fig. 4G-I). These results suggested that a prognostic signature based on five differentially expressed metabolism-related genes was associated with immunosuppressive microenvironment, and abnormalities in immune cell infiltration and differential expression of immune checkpoints were clinically relevant for early identification of patients at high risk, which might provide guidance for clinical medications.

Construction of novel prognostic model, A-IPI score, for PGI-DLBCL patients in training cohort

As previous studies have shown that metabolism-related factors are intimately associated with multiple gastrointestinal

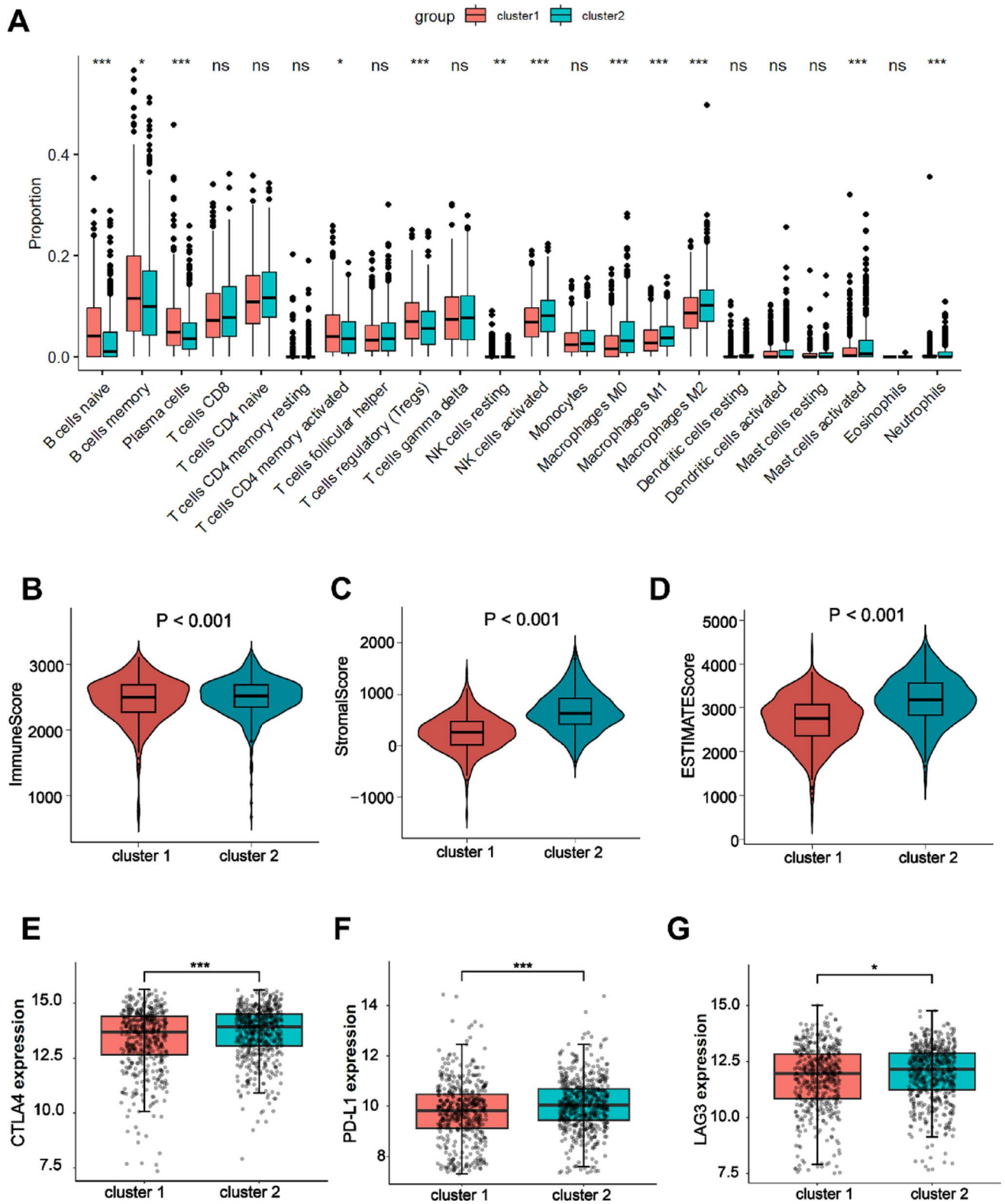

Fig. 2 Metabolism-related genes were associated with the immune microenvironment in DLBCL. (A) CIBERSORT analysis in the two clusters showed that cluster 1 had a higher level of infiltration of B cells, T cells and plasma cells, whereas cluster 2 was dominated by infiltration of NK cells, macrophages, mast cells, and neutrophils. (B-D) ESTIMATE algorithm showed significant differences in immune scores, stromal scores and ESTIMATE scores of patients in two clusters. (E-G) Expression differences of the immune checkpoints, including CTLA-4, PD-L1 and LAG-3 between the two clusters (*$p < 0.05$, **$p < 0.01$, ***$p < 0.001$)

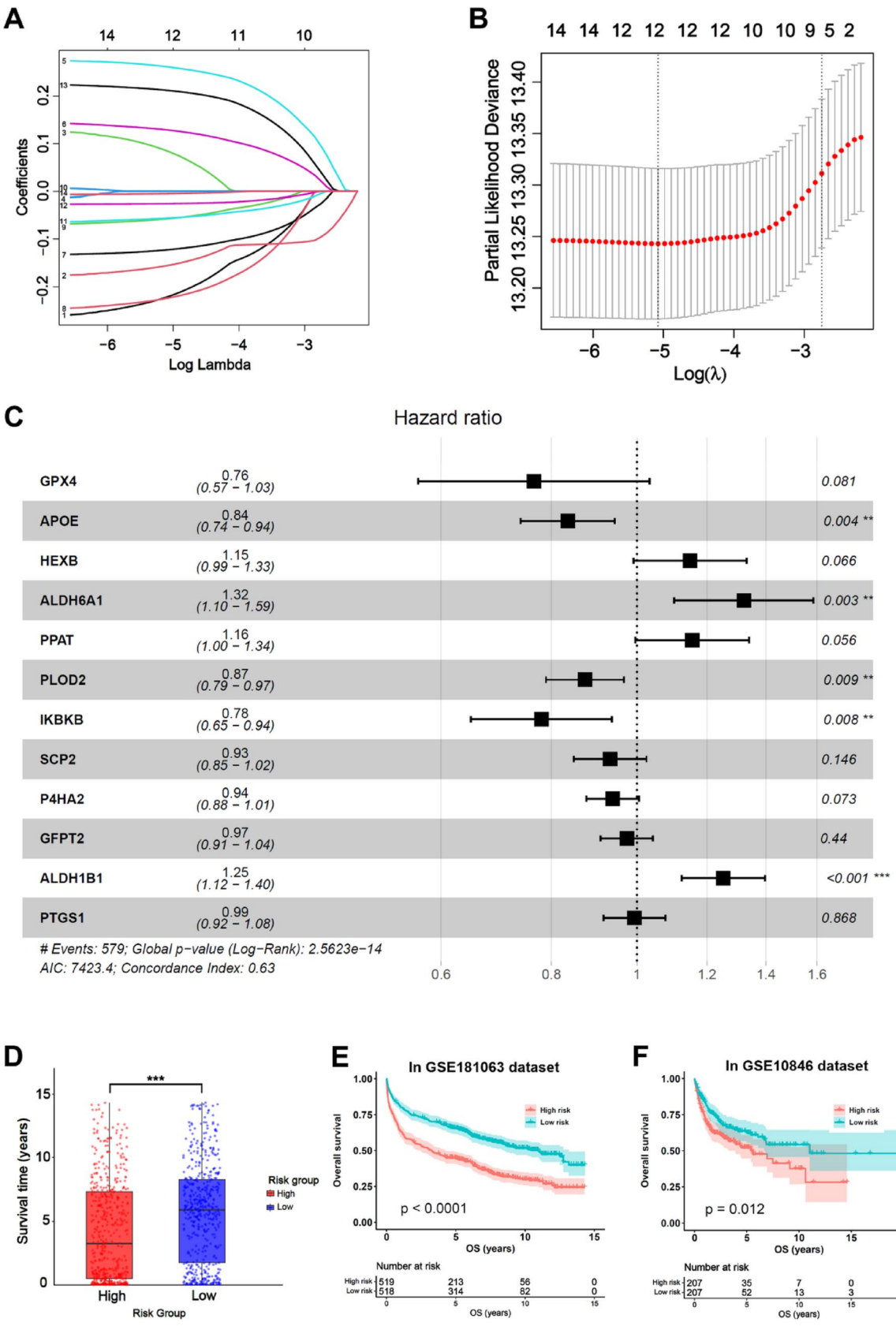
A
Coefficients
Log Lambda
B
Partial Likelihood Deviance
Log(λ)
C
Hazard ratio
GPX4 0.76 (0.57 – 1.03) 0.081
APOE 0.84 (0.74 – 0.94) 0.004 **
HEXB 1.15 (0.99 – 1.33) 0.066
ALDH6A1 1.32 (1.10 – 1.59) 0.003 **
PPAT 1.16 (1.00 – 1.34) 0.056
PLOD2 0.87 (0.79 – 0.97) 0.009 **
IKBKB 0.78 (0.65 – 0.94) 0.008 **
SCP2 0.93 (0.85 – 1.02) 0.146
P4HA2 0.94 (0.88 – 1.01) 0.073
GFPT2 0.97 (0.91 – 1.04) 0.44
ALDH1B1 1.25 (1.12 – 1.40) <0.001 ***
PTGS1 0.99 (0.92 – 1.08) 0.868
Events: 579; Global p−value (Log−Rank): 2.5623e−14
AIC: 7423.4; Concordance Index: 0.63
D
Survival time (years)
Risk group
High
Low
Risk Group
E
In GSE181063 dataset
Overall survival
p < 0.0001
OS (years)
Number at risk
F
In GSE10846 dataset
p = 0.012

Fig. 3 Construction and validation of the metabolism-related gene signature, and related immune characterization analyses. (A-B) LASSO Cox regression analysis of 14 metabolism-related genes with prognostic significance in GSE181063 dataset. (C) Multivariate forest plot of 12 metabolism-related prognostic genes showed *APOE*, *ALDH6A1*, *PLOD2*, *IKBKB* and ALDH1B1 were independent prognostic factors in GSE181063 dataset. (D) Box plots showed the difference in survival between patients with high and low risk scores. (E-F) Survival curve of GSE181063 and GSE10846 datasets verified differences in survival between high and low risk groups. (*$p < 0.05$, **$p < 0.01$, ***$p < 0.001$)

solid tumors [13–15], and PGI-DLBCL is the most common extra-nodal lymphoma, our clinical study focused on the association between metabolism-related factors and the prognosis of PGI-DLBCL patients. A total of 159 patients were included in the study, of which 102 originated in the stomach and 57 in the intestine. The clinical characteristics of patients were shown in **Supplemental Table** 3. At first, we analyzed the survival of patients with PG-DLBCL and Primary intestinal DLBCL (PI-DLBCL), and found that there was no statistically significant difference in survival between the two group ($P > 0.05$) (Fig. 5A, **Supplemental Fig.** 4 A). Therefore, we studied PG-DLBCL and PI-DLBCL as the same whole. Subsequently, we performed survival analysis of PGI-DLBCL patients who received different treatment regimens (including radiotherapy and/or chemotherapy, surgery, and surgery combined with radiotherapy and/or chemotherapy), and found that there was no significant difference ($P > 0.05$) in OS and PFS (Fig. 5B, **Supplemental Fig.** 4B).

We randomized patients into training cohort ($n = 87$) and validation cohort ($n = 72$) based on "randomizr" R package, and **Supplemental Table**4 showed that there was no statistically significant difference in the baseline levels of the two cohorts ($P > 0.05$). In univariate analysis, age ($P = 0.027$), prealbumin (PA, $P = 0.034$), apolipoprotein A (APOA, $P = 0.006$) were significantly associated with OS of PGI-DLBCL patients in training cohort (Fig. 5C). Multivariate Cox regression analysis was then performed for prognostic factors in the univariate analysis, and showed that ApoA ($P = 0.03$) was independent factor for prognosis prediction of PGI-DLBCL patients in training cohort (Fig. 5D). The Cox proportion hazard model for PGI-DLBCL patients in training cohort was shown in Table 1. Moreover, the forest plot showed that metabolism-related indicators were also associated with PFS of PGI-DLBCL in training cohort (**Supplemental Fig.**5 A). Meanwhile, we performed univariate Cox regression analyses in PG-DLBCL and PI-DLBCL, and found that APOA was correlated with the prognosis of both PG-DLBCL and PI-DLBCL patients (**Supplemental Fig.**5B-C). These results suggested that metabolism-related indicators were strongly related to survival time in PGI-DLBCL patients.

Multivariate Cox regression analysis showed that APOA had a regression coefficient (B) of − 1.808 (< 0) and a hazard ratio (HR) of 0.161 (< 1), suggesting that APOA was a protective factor for PGI-DLBCL patients. Based on the regression coefficients (B) of the multivariate Cox regression analysis, patients with APOA <1 g/L were allocated 1.5 points as a risk factor and combined it with the NCCN-IPI score, classical prognostic score systems in DLBCL, to construct a new prognostic model, A-IPI score.

A-IPI score exhibited favorable prognosis predictive efficacy in PGI-DLBCL

Using the ROC curve, we obtained the optimal cut-off value for A-IPI score, which had the best stratification with A-IPI score equal to 3. Subsequently, patients were categorized into high and low score groups based on A-IPI score, where OS and PFS were found to be significantly worse in the high score group than low score group ($P = 0.021$, $P = 0.017$) (Fig. 6A-B).

To clarify the predictive power of the A-IPI score, we assessed the score by comparing with the NCCN-IPI. The DCA and ROC curve showed better predictive ability of A-IPI score with an AUC of 0.7829 for OS and 0.7022 for PFS compared with NCCN-IPI, with an AUC of 0.6503 for OS and 0.5886 for PFS (Fig. 6C-D, **Supplemental Fig.** 5D-E). In addition, time-dependent ROC curves demonstrated that A-IPI scores had better 1-, 3-, and 5-year AUCs of 0.950, 0.805, and 0.674, respectively, compared with the NCCN-IPI scores, which had 1-, 3-, and 5-year AUCs of 0.917, 0.698, and 0.656 (Fig. 6E, **Supplemental Fig.** 6 A-B). The above results demonstrated that the A-IPI score had excellent predictive efficacy for OS and PFS of PGI-DLBCL patients in training cohort.

Based on the cutoff value of 3 obtained in training cohort, we divided the patients into high and low score groups in validation cohort. We found that the OS and PFS of the high score group were significantly worse than those of the low score group ($P = 0.012$, $P = 0.0097$) (Fig. 6F-G). In addition, ROC curve showed better predictive ability of A-IPI score with an AUC of 0.7424 in OS for validation cohort compared with NCCN-IPI, with an AUC of 0.6218 (Fig. 6H). Furthermore, time-dependent ROC curves revealed better 1-, 3-, and 5-year AUC of 0.758, 0.846, 0.826 in OS and 0.803, 0.857, 0.827 in PFS for the A-IPI score compared with the NCCN-IPI score, which had a 1-, 3-, and 5-year AUC of 0.681, 0.710, 0.693 in OS and 0.663, 0.743, 0.643 in PFS for validation cohort, respectively (Fig. 6I-J, **Supplemental Fig.** 6 C-F). The above results suggested that the A-IPI score had great prognostic efficacy for prognostic assessment in validation cohort.

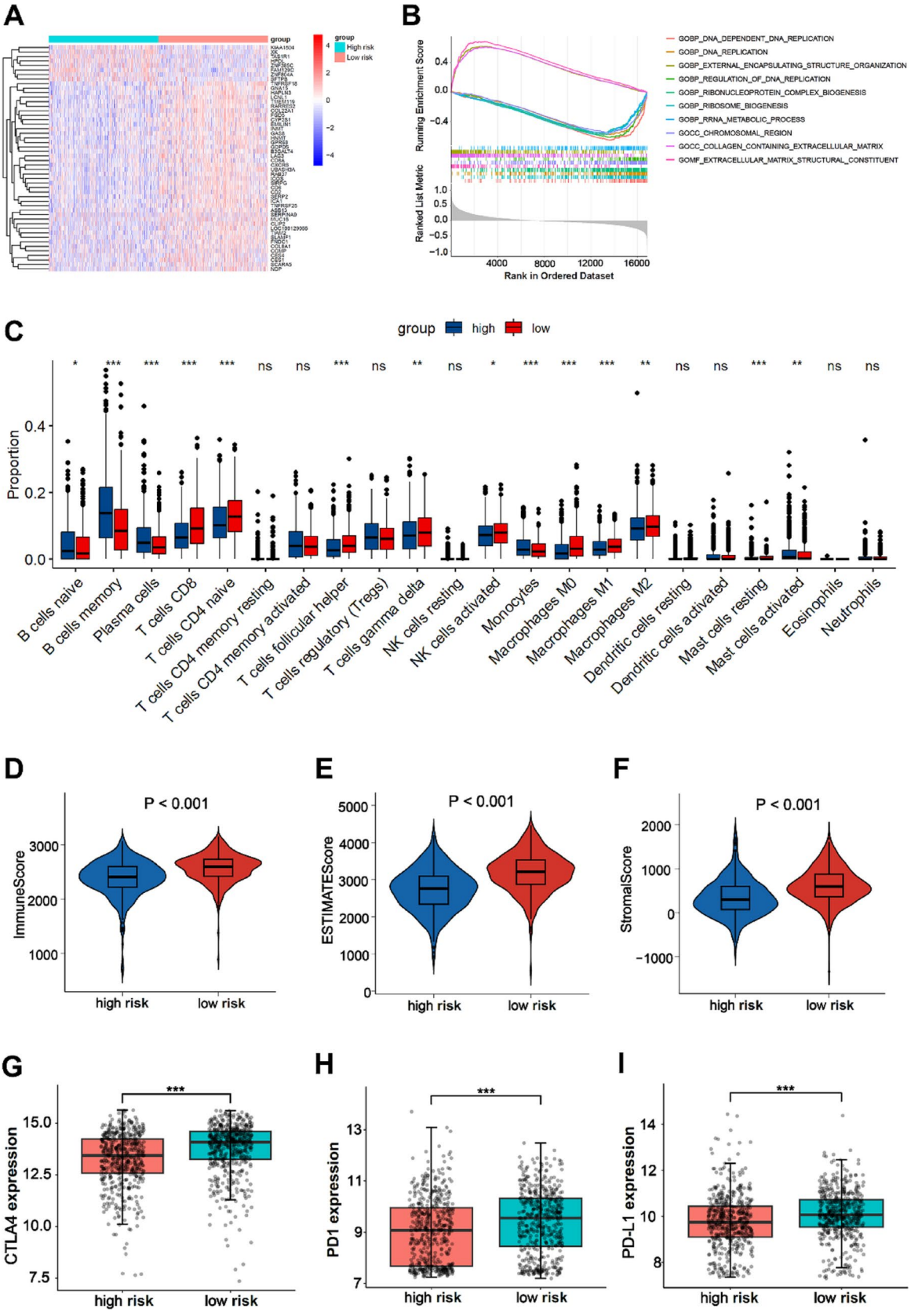
A
group
High risk
Low risk
B
GOBP_DNA_DEPENDENT_DNA_REPLICATION
GOBP_DNA_REPLICATION
GOBP_EXTERNAL_ENCAPSULATING_STRUCTURE_ORGANIZATION
GOBP_REGULATION_OF_DNA_REPLICATION
GOBP_RIBONUCLEOPROTEIN_COMPLEX_BIOGENESIS
GOBP_RIBOSOME_BIOGENESIS
GOBP_RRNA_METABOLIC_PROCESS
GOCC_CHROMOSOMAL_REGION
GOCC_COLLAGEN_CONTAINING_EXTRACELLULAR_MATRIX
GOMF_EXTRACELLULAR_MATRIX_STRUCTURAL_CONSTITUENT
Running Enrichment Score
Ranked List Metric
Rank in Ordered Dataset
C
group high low
Proportion
B cells naive
B cells memory
Plasma cells
T cells CD8
T cells CD4 naive
T cells CD4 memory resting
T cells CD4 memory activated
T cells follicular helper
T cells regulatory (Tregs)
T cells gamma delta
NK cells resting
NK cells activated
Monocytes
Macrophages M0
Macrophages M1
Macrophages M2
Dendritic cells resting
Dendritic cells activated
Mast cells resting
Mast cells activated
Eosinophils
Neutrophils
D
P < 0.001
ImmuneScore
high risk
low risk
E
P < 0.001
ESTIMATEScore
high risk
low risk
F
P < 0.001
StromalScore
high risk
low risk
G
CTLA4 expression
high risk
low risk
H
PD1 expression
high risk
low risk
I
PD-L1 expression
high risk
low risk

Fig. 4 Metabolism-related genes signature was associated with biological characteristics and immune cells infiltration in DLBCL. (A) Heatmap of the top 50 differentially expressed genes between the high and low risk groups. (B) GSEA analysis of differentially expressed genes between high and low risk groups. (C) CIBERSORT analysis in the two risk groups. (D-F) ESTIMATE algorithm showed significant differences in immune scores, ESTIMATE scores and stromal scores between two risk groups. (G-I) Expression differences of the immune checkpoints, including CTLA-4, PD-1, and PD-L1 between the two risk groups (*$p < 0.05$, **$p < 0.01$, ***$p < 0.001$)

In order to further validate the predictive efficacy of A-IPI score, we compared A-IPI score with staged-modified IPI score by ROC curves in PG-DLBCL. It was found that A-IPI score (OS, AUC = 0.6744; PFS, AUC = 0.6537) had better prognostic predictive efficacy than staged-modified IPI score (OS, AUC = 0.6266; PFS, AUC = 0.5553) (**Supplemental Fig.**7 A-B). Meanwhile, A-IPI score was compared with IPI score and Lugano stage for PI-DLBCL, and showed that the predictive efficacy of A-IPI score (OS, AUC = 0.8261; PFS, AUC = 0.7103) was superior to that of IPI score (OS, AUC = 0.7119; PFS, AUC = 0.631) and Lugano stage (OS, AUC = 0.5403; PFS, AUC = 0.5705) (**Supplemental Fig.**7 C-F). These results suggested that A-IPI score had an excellent prognostic predictive efficacy in both PG-DLBCL and PI-DLBCL.

ALDH1B1 was identified as potential prognostic biomarker and drug target in PGI-DLBCL

To further search for metabolism-related prognostic biomarkers for PGI-DLBCL, bioinformatics analysis revealed that ALDH1B1 was an independent prognostic factor in DLBCL patients. Therefore, we performed immunohistochemical analysis and drug sensitivity analysis of ALDH1B1. Immunohistochemical analysis showed that ALDH1B1 was highly expressed in PGI-DLBCL compared with reactive hyperplastic lymph node tissues (Fig. 7A). We individually analyzed the expression levels of ALDH1B1 in DLBCL and reactive hyperplastic lymph nodes in the GSE32018 dataset and found that ALDH1B1 was highly expressed in DLBCL ($P = 0.004$) (**Supplemental Fig.**8 A). In the GSE66770 dataset, we analyzed the expression levels of ALDH1B1 in PGI-DLBCL and systemic DLBCL and found that ALDH1B1 expression was upregulated in PGI-DLBCL ($P < 0.001$) (**Supplemental Fig.**8B). Subsequently, we included ALDH1B1 in a univariate analysis and found that it was associated with the OS and PFS of PGI-DLBCL (Fig. 7B, **Supplemental Fig.** 8 C). Additionally, Survival analysis showed that the high expression of ALDH1B1 was associated with worse prognosis in PGI-DLBCL (Fig. 7C-D). We analyzed the survival of patients with high and low ALDH1B1 expression in GSE181063 and GSE10846 datasets, and found that the patients with high ALDH1B1 expression had worse survival (**Supplemental Fig.**8D-E). Drug sensitivity analysis found that the group with high ALDH1B1 expression had higher sensitivity to BI-2536 and correlation analysis found that the sensitivity of patients to BI-2536 was negatively correlated with ALDH1B1 (**Supplemental Fig.**8 F-G). Furthermore, to clarify the relationship between ALDH1B1 and the immune microenvironment, we compared the immune scores and the expression levels of immune checkpoints of patients with high and low ALDH1B1 expression in GSE181063 dataset. We found that immune scores, ESTIMATE scores, and stromal scores were higher and the immune checkpoints (CTLA-4, PD-1, PD-L1) were down-regulated in ALDH1B1 high expression (**Supplemental Fig.** 9 A-F). Also, we performed KEGG enrichment analysis of DEGs in the high and low ALDH1B1 expression patients. We found that ALDH1B1 may regulate tumor development in PGI-DLBCL patients by regulating PI3K-Akt signaling pathway, Wnt signaling pathway, TGF-beta signaling pathway, Notch signaling pathway and so on (**Supplemental Fig.**9G).

In addition, to further explore the role of ALDH1B1, we examined the effect of IGUANA-1, a selective inhibitor of ALDH1B1, in DLBCL cells. Cell proliferation was reduced by the incubation with IGUANA-1 in time- and concentration-dependent manner, with the LY1 cell line showing an IC50 of 2.76 μM at 48 h (Fig. 8A-B, **Supplemental Fig.**9H). ALDH1B1 might promote lung adenocarcinoma and colon cancer progression by regulating the PI3K/AKT signaling pathway [28, 29]. Bioinformatics analysis revealed that patients with high and low ALDH1B1 expression were enriched for differential genes into the PI3K/AKT signaling pathway **(Supplemental Fig.** 9G**)**, which suggested that ALDH1B1 may promote the progression of DLBCL through the PI3K/AKT signaling pathway. Duvelisib, a PI3K inhibitor, suppresses the growth and viability of B-cell lineage tumors by inhibiting the activity of the key enzymes PI3K-δ and PI3K-γ [30]. Hence, we investigated the synergistic effect of IGUANA-1 with PI3K inhibitor duvelisib, and found that they had a high synergistic index of 24.668, which indicated an intense and stable synergistic antitumor effect of IGUANA-1 and duvelisib in DLBCL cells [31] (Fig. 8C-D). These results indicated that ALDH1B1 might be potential prognostic biomarker and drug target in PGI-DLBCL.

Discussion

Our study explored the potential role and molecular mechanisms of metabolism-related prognostic genes in DLBCL and revealed the importance of metabolism-related prognostic factors in the prognosis of PGI-DLBCL. In recent years,

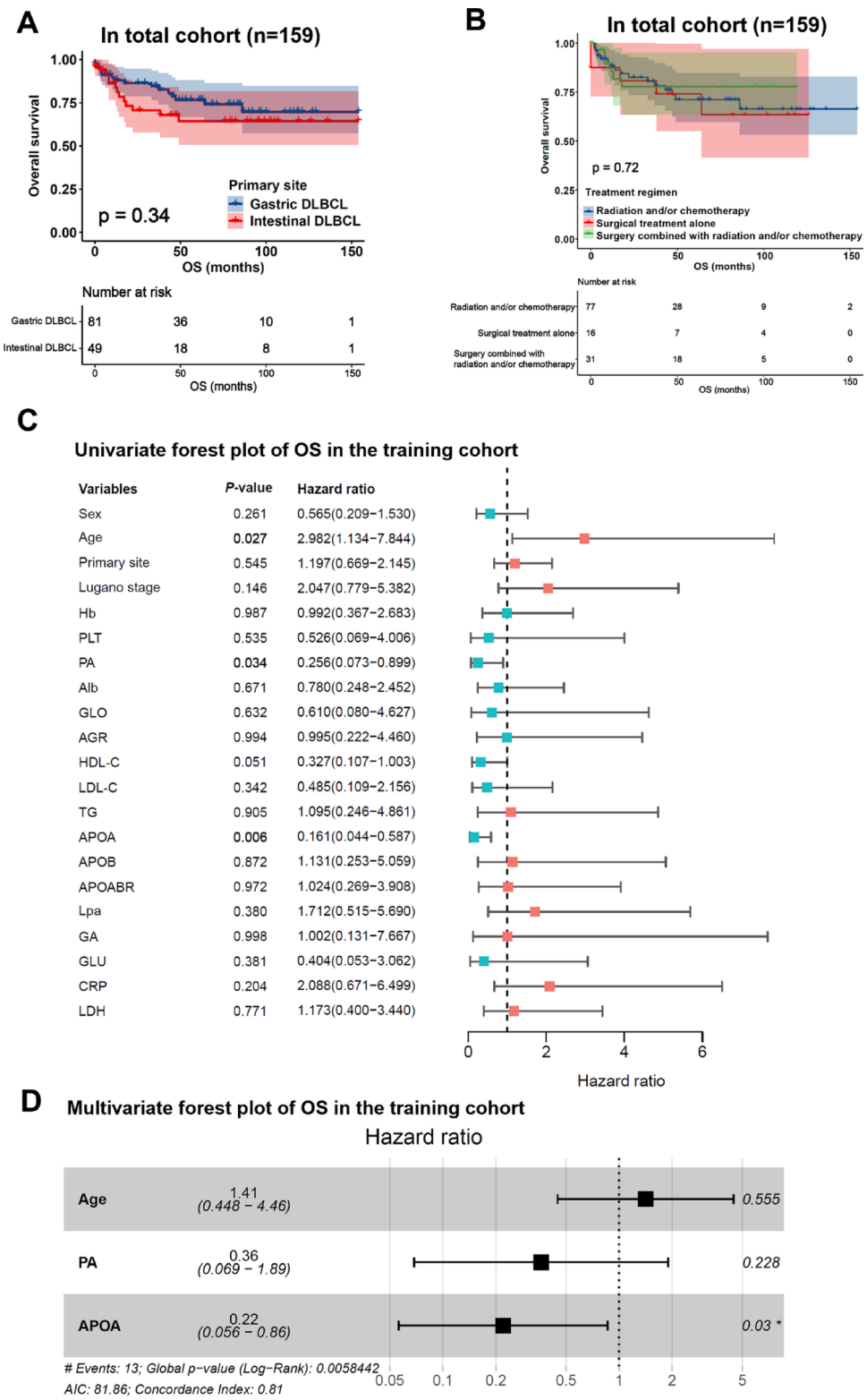

Fig. 5 Construction of A-IPI score for predicting prognosis of PGI-DLBCL patients in the training cohort. (A) Survival curves showed no difference in OS between gastric DLBCL and intestinal DLBCL in the total cohort ($n = 159$). (B) Survival curves demonstrated that OS of PGI-DLBCL patients received different treatment regimens showed no statistically significant difference ($n = 159$). (C) Forest plot based on univariate analysis showed that age, PA, APOA were significantly associated with OS of PGI-DLBCL patients in training cohort ($n = 87$). (D) Multivariate analysis of forest plot showed that APOA was independent prognostic factors of OS for PGI-DLBCL patients in training cohort. Abbreviations: AGR, albumin to globulin ratio; Alb, albumin; APOA, apolipoprotein A; APOB, apolipoprotein B; APOABR, apolipoprotein A to apolipoprotein B ratio; CRP, C-reactive protein; GA, glycated albumin; GLO, globulin; GLU, glucose; Hb, hemoglobin; HDL-C, high-density lipoprotein cholesterol; LDH, lactate dehydrogenase; LDL-C, low-density lipoprotein cholesterol; LPa, lipoprotein a; OS, overall survival; PA, prealbumin; PFS, progression-free survival; PLT, platelets; TG, triglycerides

metabolic reprogramming has become a focus of research in tumors, which has contributed to more interest in the metabolic status of tumor patients. For example, metabolic reprogramming of glucose, lipids and various amino acids promoted tumor progression in thyroid cancer cells [32, 33]. Nucleolar and spindle associated protein 1 (NUSAP1) could activate LDHA expression and promote glycolytic metabolic reprogramming by directly binding to c-Myc and HIF-1α to form a transcriptional regulatory complex, consequently promoting invasion and metastasis of pancreatic

Table 1 Univariate and multivariate analysis of OS in training cohort of primary Gastrointestinal diffuse large B-cell lymphoma patients

Parameters		Univariate analysis				Multivariate analysis			
		B	SE	HR (95% CI)	*P*-value	B	SE	HR (95% CI)	*P*-value
Sex	Female vs. Male	0.569	0.508	0.565 (0.209, 1.530)	0.261				
Age, years	≥ 60 vs. < 60	1.088	0.493	2.982 (1.134, 7.884)	**0.027**	0.331	0.587	1.414 (0.448, 4.465)	0.555
Primary site	Gastric vs. Intestinal	0.177	0.297	1.197 (0.669, 2.145)	0.545				
Lugano stage	IE, IIE vs. IIIE, IV	0.719	0.493	2.047 (0.779, 5.382)	0.146				
Hb, g/L	≥ 115 vs. < 115	− 0.010	0.508	0.992 (0.367, 2.683)	0.987				
PLT, 10^9/L	> 125 vs. ≤ 125	− 0.648	1.036	0.526 (0.069, 4.006)	0.535				
PA, mg/L	≥ 180 vs. < 180	− 1.353	0.641	0.256 (0.073, 0.899)	**0.034**	− 1.011	0.847	0.364 (0.069, 1.892)	0.228
Alb, g/L	≥ 40 vs. < 40	− 0.245	0.585	0.780 (0.248, 2.452)	0.671				
GLO, g/L	≥ 20 vs. < 20	− 0.499	1.034	0.610 (0.080, 4.627)	0.632				
AGR	≥ 1.2 vs. < 1.2	− 0.001	0.766	0.995 (0.222, 4.440)	0.994				
HDL-C, mmol/L	≥ 1.04 vs. < 1.04	− 1.118	0.572	0.327 (0.107, 1.003)	0.051				
LDL-C, mmol/L	> 3.37 vs. ≤ 3.37	− 0.723	0.761	0.485 (0.109, 2.156)	0.342				
TG, mmol/L	> 1.7 vs. ≤ 1.7	0.089	0.761	1.095 (0.246, 4.861)	0.905				
APOA, g/L	≥ 1 vs. < 1	− 1.808	0.659	0.161 (0.044, 0.587)	**0.006**	− 1.496	0.696	0.224 (0.056, 0.860)	**0.030**
APOB, g/L	> 1.1 vs. ≤ 1.1	0.118	0.764	1.131 (0.253, 5.058)	0.872				
APOABR	≥ 1 vs. < 1	0.326	0.597	1.024 (0.269, 3.908)	0.972				
LPa, g/L	> 0.3 vs. ≤ 0.3	0.452	0.613	1.712 (0.515, 5.690)	0.380				
GA%	> 16 vs. ≤ 16	− 0.098	1.039	1.002 (0.131, 7.667)	0.998				
GLU, mmol/L	> 6.1 vs. ≤ 6.1	− 0.901	1.033	0.404 (0.053, 3.062)	0.381				
CRP, mg/L	> 10 vs. ≤ 10	0.735	0.579	2.088 (0.671, 6.499)	0.204				
LDH, U/L	> 250 vs. ≤ 250	0.159	0.549	1.173 (0.400, 3.437)	0.771				

Abbreviations: AGR, albumin to globulin ratio; Alb, albumin; APOA, apolipoprotein A; APOB, apolipoprotein B; APOABR, apolipoprotein A to apolipoprotein B ratio; CRP, C-reactive protein; GA, glycated albumin; GLO, globulin; GLU, glucose; Hb, hemoglobin; HDL-C, high-density lipoprotein cholesterol; HR, hazard ratio; LDH, lactate dehydrogenase; LDL-C, low-density lipoprotein cholesterol; LPa, lipoprotein a; PA, prealbumin; PLT, platelets; SE, standard error; TG, triglycerides

ductal adenocarcinoma [34]. A study on adrenocortical carcinoma found that metabolic heterogeneity of nutrients such as carbohydrates, lipids, and proteins affected patient prognosis [35]. The altered metabolism of amino acids and lipids in the tumor resulted in dysregulation of anti-tumor immune response and the development of resistance to anti-PD-1/PD-L1 therapy [36]. In addition, a large number of studies have shown that the poor prognosis of tumor patients was closely related to the metabolic status of patients [37–39]. Our study analyzed the relationship between metabolism-related factors and survival of PGI-DLBCL patients, and innovatively revealed the independent predictive value of metabolism-related factors for PGI-DLBCL. In addition, a novel model (A-IPI score) combining APOA and NCCN-IPI was developed, which was confirmed to be more effective than NCCN-IPI in PGI-DLBCL patients. These results provided powerful scientific evidence for the risk assessment and prognostic stratification of initially diagnosed PGI-DLBCL. However, since our study was conducted with a small sample in a single center, the limited number of patients and lack of ethnic diversity may lead to biased results and weaken credibility. Therefore, multi-center, large sample and long-term follow-up studies are needed for model validation and optimization in the future.

Recent studies have found that metabolism-related genes could be used as prognostic markers in a variety of tumors [40, 41]. In a study of gliomas, glucose metabolism-related genes were found to promote tumor progression [42], indirectly confirming reprogramming of glucose metabolism as a promising strategy for the treatment of gliomas [43]. In addition, prognostic models of head and neck squamous cell carcinoma based on glucose metabolism-related genes and lipid metabolism-related genes have been developed [44, 45]. Moreover, amino acid metabolism-related genes have been found to be associated with the immune microenvironment in AML patients, which could predict the prognosis and response to immunotherapy in AML patients [46]. The above studies indicated the prognostic role of metabolism-related genes in a variety of tumors. In this study, we analyzed the relationship between metabolism-related prognostic genes and the prognosis of DLBCL patients, established a prognostic signature based on five metabolism-related prognostic genes, and found that the score was closely related to the immunosuppressive microenvironment. The findings demonstrated the role and potential mechanisms of metabolism-related genes in the prognostic assessment of DLBCL, but the specific mechanisms involved need to be explored in further studies.

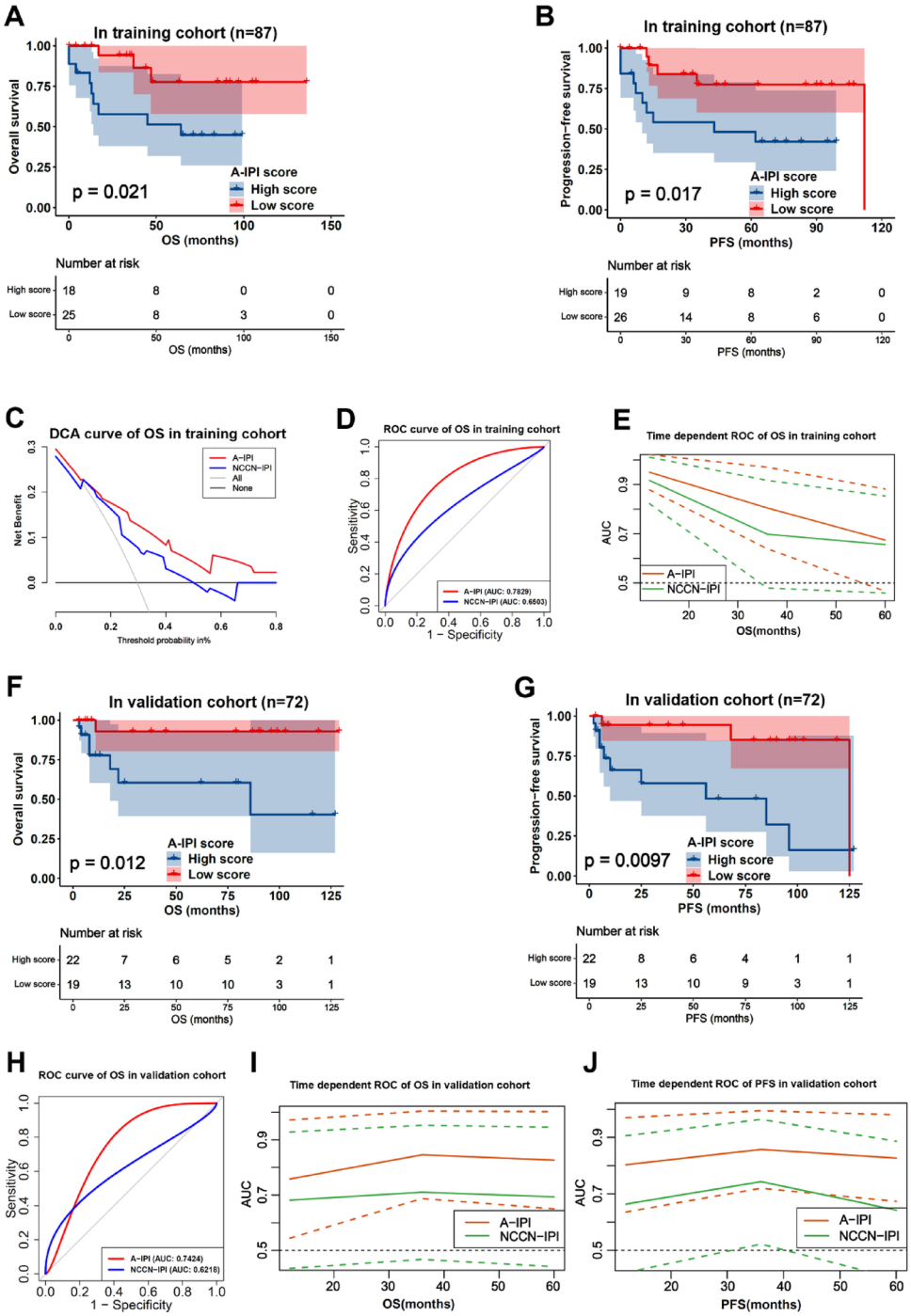

Fig. 6 A-IPI score exhibited favorable efficacy for predicting prognosis of PGI-DLBCL patients in training and validation cohorts. (A-B) Kaplan-Meier curves of OS and PFS showed that PGI-DLBCL patients in high score group had worse survival in training cohort ($n = 87$). (C) Decision curve analysis showed that A-IPI score was more useful than NCCN-IPI score for clinical decision making in training cohort due to higher net benefit. (D) ROC curves showed that the A-IPI score had better prognostic ability than the NCCN-IPI score for predicting OS in training cohort. (E) The 1-, 3-, and 5-year time-dependent ROC showed that the A-IPI score had higher discriminatory power than the NCCN-IPI score for predicting OS in training cohort. (F-G) Kaplan-Meier curves of OS and PFS showed that PGI-DLBCL patients in high score group had worse survival in validation cohort. (H) ROC curves showed that the A-IPI score model had better prognostic ability than the NCCN-IPI score for predicting OS in validation cohort. (I-J) The 1-, 3-, and 5-year time-dependent ROC revealed that the A-IPI score had higher discriminatory power than the NCCN-IPI for predicting OS and PFS in validation cohort

Metabolic reprogramming has been identified as an important feature of immune cell activation, and immune cells have different metabolic properties that affect their immune function [47–49]. As $CD8^+$ T cells have been considered to be important immune cells for killing tumor cells [50], glucose deprivation in gastric cancer cells caused $CD8^+$ T cells to exhibit functional exhaustion with impaired proliferation, cytokine production and metabolism [51], leading to the inhibition of killing ability of $CD8^+$ T cells. Several studies have shown that amino acid metabolism promoted the expression of immune checkpoints and enhanced the immunosuppressive effects of Tregs, thereby facilitating immune escape of tumors. For example, limiting glutamine intake in the body led to upregulation of PD-L1 in lung cancer and colon cancer, which inhibited T cell activity [52]. Conversely, restoring glutamine intake upregulated PD-L1 expression and restored it to normal levels in renal cancer [53]. In addition, indoleamine 2, 3-dioxyge-nase

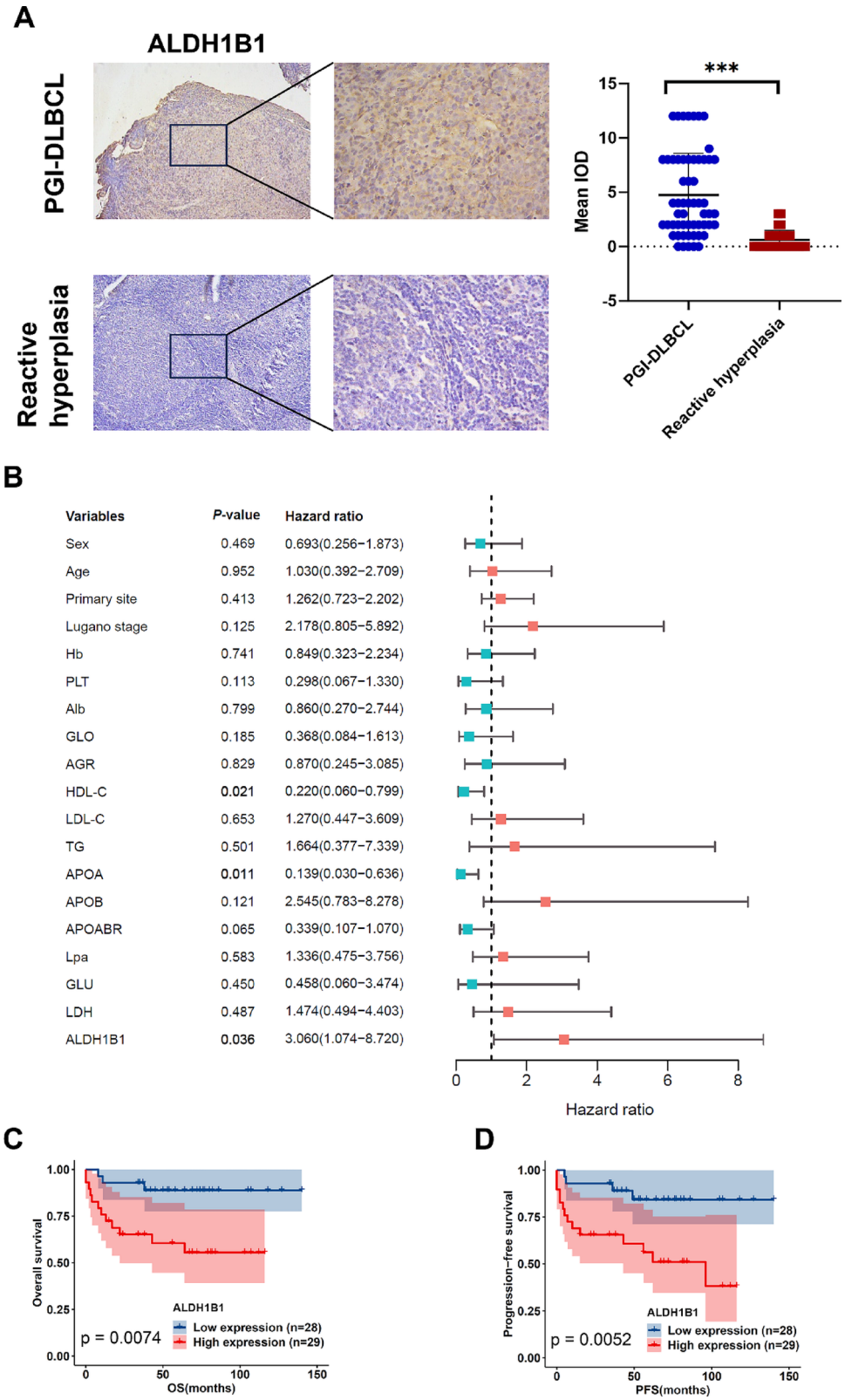

Fig. 7 High expression of ALDH1B1 was associated with worse prognosis in PGI-DLBCL. (A) Immunohistochemistry showed that ALDH1B1 was highly expressed in PGI-DLBCL ($n = 57$) compared with reactive hyperplastic tissues ($n = 30$). (B) Forest plot based on univariate analysis showed that ALDH1B1 was associated with the OS of PGI-DLBCL ($n = 57$). (C-D) Survival analysis showed that PGI-DLBCL patients in high ALDH1B1 expression group had worse prognosis ($n = 57$)

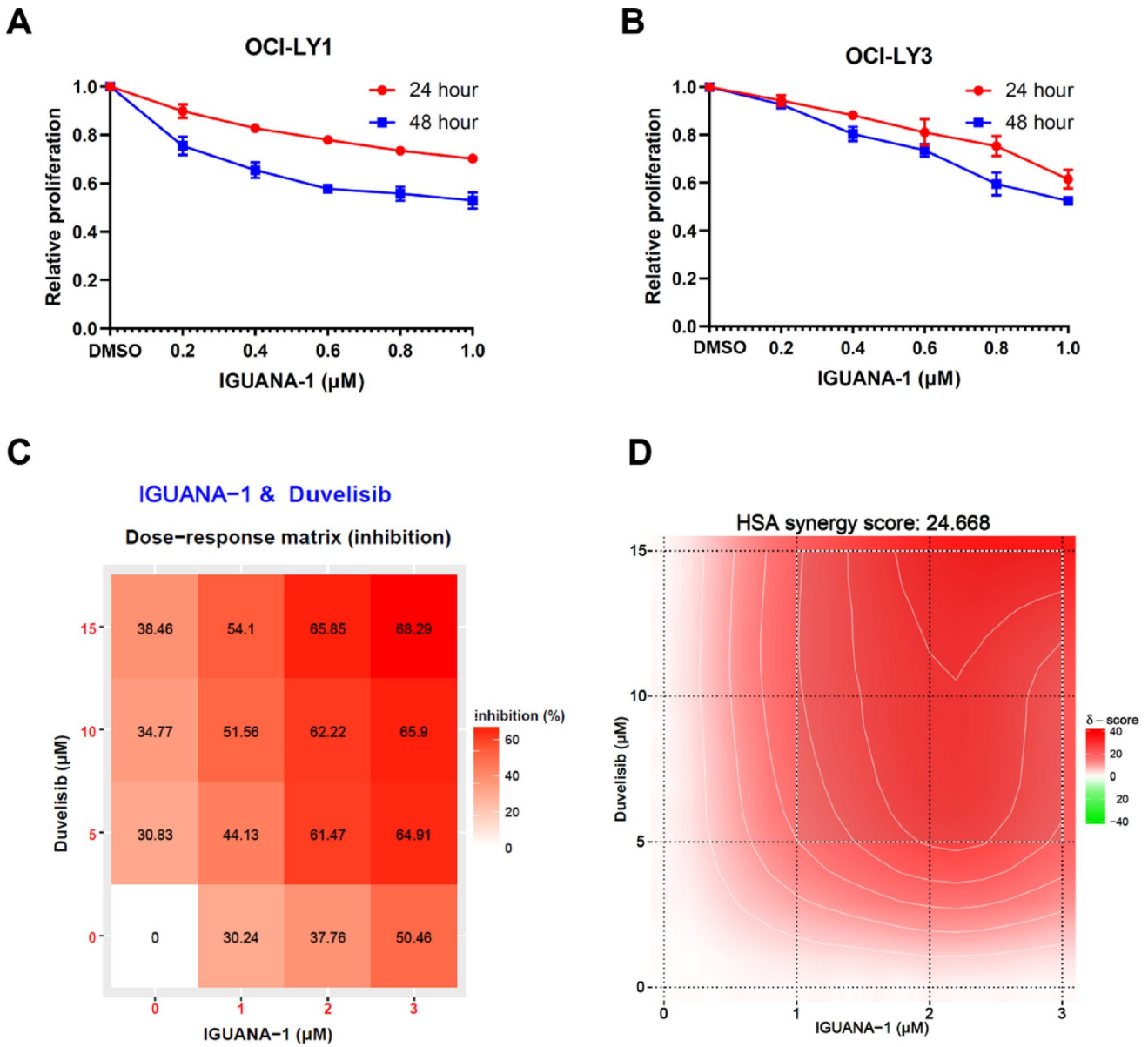

Fig. 8 ALDH1B1 inhibitor IGUANA-1 inhibited cell proliferation and exerted synergistic effect with PI3K inhibitor duvelisib in DLBCL. (A-B) IGUANA-1 decreased cell proliferation in DLBCL in time- and concentration-dependent manner. (C-D) IGUANA-1 exerted synergistic anti-tumor effect with PI3K inhibitor duvelisib in DLBCL

(IDO), a key enzyme in the tryptophan metabolic pathway, upregulated the expression of PD-L1 through activation of Tregs and enhanced the immunosuppressive effects of Tregs through PD-1/PD-L1 interaction [54, 55]. A study of gliomas found that patients with high expression of fatty acid metabolism-related genes also had high expression of CTLA-4 and PD-1, and were sensitive to anti-CTLA-4 and anti-PD-1/PD-L1 immunotherapy [56]. In our study, we found that there were significant differences in immune cell infiltration, immune scores, and expression levels of immune checkpoints between the two groups classified by metabolism-related gene prognostic signature, suggesting that metabolic reprogramming affected immune status in the tumor microenvironment and differential sensitivity to immunotherapy in DLBCL patients. The above results provided guidance for the immunotherapy of tumor patients in the clinic, but a large number of studies are still needed to explore the specific mechanisms in the future.

The gastrointestinal tract is the site of direct absorption of many substances such as glucose, amino acids, and fatty acids, and the development of PGI-DLBCL may interfere with the absorption and subsequent metabolism of nutrients in tumor patients. Currently, the treatment of PGI-DLBCL tends to be the combination of chemotherapy,

supplemented by radiotherapy or surgery. Although the majority of PGI-DLBCL patients are sensitive to chemotherapy, some patients still exhibit disease recurrence and drug resistance. Furthermore, the lack of specific clinical manifestations and the complexity of pathological features of PGI-DLBCL make it difficult to diagnose and treat early [57, 58]. Therefore, identifying effective prognostic factors can help to recognize high-risk patients early, develop individualized treatment strategies and improve the prognosis of PGI-DLBCL patients. In this study, we identified metabolism-related prognostic factors, constructed a metabolism-related prognostic model A-IPI score, and demonstrated its advantages in risk stratification and prognostic assessment of PGI-DLBCL by ROC curves, DCA and time-dependent ROC curves. Furthermore, we demonstrated that ALDH1B1 was a promising biomarker guiding prognostic prediction and drug sensitivity in PGI-DLBCL. In summary, these results showed that the novel prognostic model was effective in the prognostic assessment of PGI-DLBCL patients. The exploration of the potential prognostic biomarkers and molecular mechanisms of metabolism-related prognostic genes in PGI-DLBCL could provide a guideline for future multicenter large-sample studies.

Acetaldehyde dehydrogenase (ALDH) is a family of NAD(P)+-dependent enzymes that oxidizes endogenous and exogenous aldehydes to the corresponding carboxylic acids. Increased ALDH activity has been found in multiple myeloma, myeloid leukemia, and many solid cancers [59, 60]. ALDH1B1, a member of the ALDH superfamily, has been identified as an important mitochondrial enzyme for ethanol degradation in vivo [61]. Current studies have found that ALDH1B1 is closely associated with the development of diabetes and different kinds of tumors [62–65]. For example, ALDH1B1 was found to be overexpressed in pancreatic cancer cells and associated with tumor-initiating cells in pancreatic ductal adenocarcinoma [64]. Moreover, ALDH1B1 affected the progression of colorectal tumors and could be used as a potential prognostic biomarker for patients [63, 66]. In addition, ALDH1B1 positively regulated Wnt/β-catenin, Notch and PI3K/Akt signaling pathways to promote colon tumor progression [29]. Updated research found that colorectal tumor could be targeted by small molecule inhibitors of ALDH1B1 [67]. A study on lung adenocarcinoma found that ALDH1B1 promoted EMT by increasing the levels of SNAI1/2, ZEB2, and TWIST1, consequently decreasing the expression of CDH1 (E-calmodulin), which promoted the progression of lung adenocarcinoma cells [28]. In our study, bioinformatics analysis and immunohistochemistry revealed that ALDH1B1 was highly expressed in PGI-DLBCL compared to reactive hyperplastic lymph node tissues, and the high ALDH1B1 expression group of PGI-DLBCL had worse survival, suggesting that ALDH1B1 was closely associated with the development of PGI-DLBCL. Cell proliferation assays showed that ALDH1B1 inhibitor IGUANA-1 suppressed the growth of DLBCL cells, indicating the potential of ALDH1B1 as drug target in DLBCL treatment. Drug sensitivity analysis revealed that the expression level of ALDH1B1 was closely associated with drug sensitivity in PGI-DLBCL patients, and ALDH1B1 inhibitor IGUANA-1 exerted synergistic anti-tumor effects with PI3K inhibitor duvelisib. Also, we performed enrichment analysis of DEGs in patients with high and low ALDH1B1 expression. It was found that ALDH1B1 may promote tumor progression in PGI-DLBCL patients by regulating PI3K-Akt, Wnt, and other signaling pathways. These results suggested that ALDH1B1 might serve as a potential prognostic marker and drug target for PGI-DLBCL. Moreover, the expression level of ALDH1B1 might provide medication guidance for the pharmacological treatment of PGI-DLBCL patients, which needs to be explored in further studies.

In addition, our study has some limitations. Firstly, our analysis based on the GEO database lacked information on survival in PGI-DLBCL, which may lead to bias in our constructed metabolism-related genes prognostic signature in assessing the prognosis of PGI-DLBCL. Secondly, the sample of this study was derived from a single center and the sample size was limiting, which may lead to biased results. Thirdly, our study lacked an external validation cohort for the model. Therefore, we need to conduct multicenter and large-sample studies to validate the model and deeply investigate the mechanism of metabolism-related genes, providing more effective strategies for precise risk stratification and targeted therapy in PGI-DLBCL patients.

In conclusion, bioinformatic analysis explored the potential mechanisms by which metabolism-related genes affect the prognosis of DLBCL, and established prognostic risk stratification based on metabolism-related genes, which provided a theoretical basis for future research. Additionally, A-IPI score was found to be an accessible and effective prognostic model for PGI-DLBCL patients. Compared with the NCCN-IPI, A-IPI score showed better assessment results, providing a strong basis for risk stratification and prognostic assessment of patients with initial diagnosis of PGI-DLBCL, and guiding the early treatment of patients. Metabolism-related ALDH1B1 was identified as potential prognostic biomarker and drug target in PGI-DLBCL, which provided reference value for clinical treatment of PGI-DLBCL. Collectively, our findings revealed the correlation between metabolism-related factors and prognosis in PGI-DLBCL and emphasized the significance of metabolism-related genes, especially ALDH1B1, in the clinical management of PGI-DLBCL.

Supplementary Information The online version contains supplementary material available at https://doi.org/10.1007/s10495-025-02112-1.

Acknowledgements Not applicable.

Author contributions QQQ and SFH conceived and designed the study, reviewed the data, and revised the manuscript. QQQ and BYL performed the experiments. QQQ, JJS and WYS and XLZ processed the experimental data and prepared the manuscript figures. QQQ and SFH wrote the main part of the manuscript. XW and XSF discussed the results and reviewed the manuscript. All authors read and approved the final manuscript.

Funding sources This study was funded by National Natural Science Foundation (No.82270200, No.82070203, No.81770210 and No.82400231); Taishan Scholars Program of Shandong Province; Shandong Provincial Engineering Research Center of Lymphoma; Key Research and Development Program of Shandong Province (No.2018CXGC1213); Academic Promotion Programme of Shandong First Medical University (No. 2019QL018); Translational Research Grant of NCRCH (No.2021WWB02, No.2020ZKMB01); China Postdoctoral Science Foundation (No. 2023M741506); Shandong Provincial Natural Science Foundation (No. ZR2023QH193, No.ZR2023MH376).

Data availability No datasets were generated or analysed during the current study.

Declarations

Ethics statement The study was conducted in accordance with the Declaration of Helsinki. The study was approved by the Research Ethics Committee in Shandong Provincial Hospital. Informed consent was waived because of its retrospective nature.

Conflict of interest Statement
The authors have no competing interests to declare that are relevant to the content of this article.

References

1. Sehn LH, Gascoyne RD (2015) Diffuse large B-cell lymphoma: optimizing outcome in the context of clinical and biologic heterogeneity. Blood 125:22–32. https://doi.org/10.1182/blood-2014-05-577189
2. Howell JM, Auer-Grzesiak I, Zhang J, Andrews CN, Stewart D, Urbanski SJ (2012) Increasing incidence rates, distribution and histological characteristics of primary Gastrointestinal non-Hodgkin lymphoma in a North American population. Can J Gastroenterol 26:452–456. https://doi.org/10.1155/2012/480160
3. Peng JC, Zhong L, Ran ZH (2015) Primary lymphomas in the Gastrointestinal tract. J Dig Dis 16:169–176. https://doi.org/10.1111/1751-2980.12234
4. Ramachandran P, Sahni S, Wang JC (2019) De Novo CD5+Primary Gastrointestinal diffuse large B-Cell lymphoma: challenges with treatment and clinical course. J Investig Med High Impact Case Rep 7:2324709619893546. https://doi.org/10.1177/2324709619893546
5. Lightner AL, Shannon E, Gibbons MM, Russell MM (2016) Primary Gastrointestinal Non-Hodgkin's lymphoma of the small and large intestines: a systematic review. J Gastrointest Surg 20:827–839. https://doi.org/10.1007/s11605-015-3052-4
6. Shen Y, Ou J, Wang B, Wang L, Xu J, Cen X (2021) Influence of severe Gastrointestinal complications in primary Gastrointestinal diffuse large B-Cell lymphoma. Cancer Manag Res 13:1041–1052. https://doi.org/10.2147/CMAR.S295671
7. Zhou Z, Sehn LH, Rademaker AW, Gordon LI, Lacasce AS, Crosby-Thompson A, Vanderplas A, Zelenetz AD, Abel GA, Rodriguez MA, Nademanee A, Kaminski MS, Czuczman MS, Millenson M, Niland J, Gascoyne RD, Connors JM, Friedberg JW, Winter JN (2014) An enhanced international prognostic index (NCCN-IPI) for patients with diffuse large B-cell lymphoma treated in the rituximab era. Blood 123:837–842. https://doi.org/10.1182/blood-2013-09-524108
8. Cortelazzo S, Rossi A, Roggero F, Oldani E, Zucca E, Tondini C, Ambrosetti A, Pasini F, Pinotti G, Bertini M, Vitolo U, Busetto M, Gianni L, Cavalli F, Barbui T (1999) Stage-modified international prognostic index effectively predicts clinical outcome of localized primary gastric diffuse large B-cell lymphoma. International extranodal lymphoma study group (IELSG). Ann Oncol 10:1433–1440. https://doi.org/10.1023/a:1008351427601
9. Diamantidis MD, Papaioannou M, Hatjiharissi E (2021) Primary gastric non-Hodgkin lymphomas: recent advances regarding disease pathogenesis and treatment. World J Gastroenterol 27:5932–5945. https://doi.org/10.3748/wjg.v27.i35.5932
10. Quayle FJ, Lowney JK (2006) Colorectal lymphoma. Clin Colon Rectal Surg 19:49–53. https://doi.org/10.1055/s-2006-942344
11. Kang HJ, Lee HH, Jung SE, Park KS, O JH, Jeon YW, Choi BO, Cho SG (2020) Pattern of failure and optimal treatment strategy for primary gastric diffuse large B-cell lymphoma treated with R-CHOP chemotherapy. PLoS ONE 15:e0238807. https://doi.org/10.1371/journal.pone.0238807
12. Vanheel H, Farre R (2013) Changes in Gastrointestinal tract function and structure in functional dyspepsia. Nat Rev Gastroenterol Hepatol 10:142–149. https://doi.org/10.1038/nrgastro.2012.255
13. Nagel G, Bjorge T, Jaensch A, Peter RS, Haggstrom C, Lang A, Engeland A, Teleka S, Jirstrom K, Lindquist D, Stattin P, Ulmer H, Concin H, Stocks T (2021) Metabolic factors and the risk of small intestine cancers: pooled study of 800 000 individuals in the metabolic syndrome and cancer project. Int J Cancer 149:66–74. https://doi.org/10.1002/ijc.33530
14. Papadimitriou N, Gunter MJ, Murphy N, Gicquiau A, Achaintre D, Brezina S, Gumpenberger T, Baierl A, Ose J, Geijsen A, van Roekel EH, Gsur A, Gigic B, Habermann N, Ulrich CM, Kampman E, Weijenberg MP, Ueland PM, Kaaks R, Katzke V, Krogh V, Bueno-de-Mesquita B, Ardanaz E, Travis RC, Schulze MB, Sanchez MJ, Colorado-Yohar SM, Weiderpass E, Scalbert A, Keski-Rahkonen P (2021) Circulating Tryptophan metabolites and risk of colon cancer: results from case-control and prospective cohort studies. Int J Cancer 149:1659–1669. https://doi.org/10.1002/ijc.33725

15. Wang S, Li M, Yan L, He M, Lin H, Xu Y, Wan Q, Qin G, Chen G, Xu M, Wang G, Qin Y, Luo Z, Tang X, Wang T, Zhao Z, Xu Y, Chen Y, Huo Y, Hu R, Ye Z, Dai M, Shi L, Gao Z, Su Q, Mu Y, Zhao J, Chen L, Zeng T, Yu X, Li Q, Shen F, Chen L, Zhang Y, Wang Y, Deng H, Liu C, Wu S, Yang T, Li D, Ning G, Wu T, Wang W, Bi Y, Lu J, Group CS (2022) Metabolomics study reveals systematic metabolic dysregulation and early detection markers associated with incident pancreatic cancer. Int J Cancer 150:1091–1100. https://doi.org/10.1002/ijc.33877
16. Jia Y, Wan M, Shen Y, Wang J, Luo X, He M, Bai R, Xiao W, Zhang X, Ruan J (2025) Predictive nomogram integrating radiomics and multi-omics for improved prognosis-model in cholangiocarcinoma. Clin Transl Med 15:e70171. https://doi.org/10.1002/ctm2.70171
17. Icard P, Lincet H (2016) The reduced concentration of citrate in cancer cells: an indicator of cancer aggressiveness and a possible therapeutic target. Drug Resist Updat 29:47–53. https://doi.org/10.1016/j.drup.2016.09.003
18. Cao X, Hou J, An Q, Assaraf YG, Wang X (2020) Towards the overcoming of anticancer drug resistance mediated by p53 mutations. Drug Resist Updat 49:100671. https://doi.org/10.1016/j.drup.2019.100671
19. Shahar N, Larisch S (2020) Inhibiting the inhibitors: targeting anti-apoptotic proteins in cancer and therapy resistance. Drug Resist Updat 52:100712. https://doi.org/10.1016/j.drup.2020.100712
20. Sommermann TG, O'Neill K, Plas DR, Cahir-McFarland E (2011) IKKbeta and NF-kappaB transcription govern lymphoma cell survival through AKT-induced plasma membrane trafficking of GLUT1. Cancer Res 71:7291–7300. https://doi.org/10.1158/0008-5472.CAN-11-1715
21. Blachly JS, Baiocchi RA (2014) Targeting PI3-kinase (PI3K), AKT and mTOR axis in lymphoma. Br J Haematol 167:19–32. https://doi.org/10.1111/bjh.13065
22. DeBerardinis RJ, Lum JJ, Hatzivassiliou G, Thompson CB (2008) The biology of cancer: metabolic reprogramming fuels cell growth and proliferation. Cell Metab 7:11–20. https://doi.org/10.1016/j.cmet.2007.10.002
23. Lewin KJ, Ranchod M, Dorfman RF (1978) Lymphomas of the Gastrointestinal tract: a study of 117 cases presenting with Gastrointestinal disease. Cancer 42:693–707.
24. Li SS, Zhai XH, Liu HL, Liu TZ, Cao TY, Chen DM, Xiao LX, Gan XQ, Cheng K, Hong WJ, Huang Y, Lian YF, Xiao J (2022) Whole-exome sequencing analysis identifies distinct mutational profile and novel prognostic biomarkers in primary Gastrointestinal diffuse large B-cell lymphoma. Exp Hematol Oncol 11:71. https://doi.org/10.1186/s40164-022-00325-7
25. Yang Y, Yang Y, Liu J, Zeng Y, Guo Q, Guo J, Guo L, Lu H, Liu W (2022) Establishment and validation of a carbohydrate metabolism-related gene signature for prognostic model and immune response in acute myeloid leukemia. Front Immunol 13:1038570. https://doi.org/10.3389/fimmu.2022.1038570
26. Li J, Zhang S, Chen S, Yuan Y, Zuo M, Li T, Wang Z, Liu Y (2023) Lipid metabolism-related gene signature predicts prognosis and depicts tumor microenvironment immune landscape in gliomas. Front Immunol 14:1021678. https://doi.org/10.3389/fimmu.2023.1021678
27. Xie Y, Chen H, Fang JY (2022) Amino acid metabolism-based molecular classification of colon adenocarcinomavia in Silico analysis. Front Immunol 13:1018334. https://doi.org/10.3389/fimmu.2022.1018334
28. Tsochantaridis I, Brisimis D, Tsifintaris M, Anastasiadou A, Lazos E, Ermogenous A, Christou S, Antonopoulou N, Panayiotidis MI, Koukourakis MI, Giatromanolaki A, Pappa A (2024) Exploring the role and pathophysiological significance of aldehyde dehydrogenase 1B1 (ALDH1B1) in human lung adenocarcinoma. Int J Mol Sci. https://doi.org/10.3390/ijms251910301
29. Singh S, Arcaroli J, Chen Y, Thompson DC, Messersmith W, Jimeno A, Vasiliou V (2015) ALDH1B1 is crucial for colon tumorigenesis by modulating Wnt/beta-Catenin, Notch and PI3K/Akt signaling pathways. PLoS ONE 10:e0121648. https://doi.org/10.1371/journal.pone.0121648
30. Iannello A, Vitale N, Coma S, Arruga F, Chadburn A, Di Napoli A, Laudanna C, Allan JN, Furman RR, Pachter JA, Deaglio S, Vaisitti T (2021) Synergistic efficacy of the dual PI3K-delta/gamma inhibitor Duvelisib with the Bcl-2 inhibitor venetoclax in Richter syndrome PDX models. Blood 137:3378–3389. https://doi.org/10.1182/blood.2020010187
31. Vlot AHC, Aniceto N, Menden MP, Ulrich-Merzenich G, Bender A (2019) Applying synergy metrics to combination screening data: agreements, disagreements and pitfalls. Drug Discov Today 24:2286–2298. https://doi.org/10.1016/j.drudis.2019.09.002
32. Duan SL, Wu M, Zhang ZJ, Chang S (2023) The potential role of reprogrammed glucose metabolism: an emerging actionable codependent target in thyroid cancer. J Transl Med 21:735. https://doi.org/10.1186/s12967-023-04617-2
33. Nagayama Y, Hamada K (2022) Reprogramming of cellular metabolism and its therapeutic applications in thyroid cancer. Metabolites. https://doi.org/10.3390/metabo12121214
34. Chen M, Cen K, Song Y, Zhang X, Liou YC, Liu P, Huang J, Ruan J, He J, Ye W, Wang T, Huang X, Yang J, Jia Y, Liang X, Shen P, Wang Q, Liang T (2023) NUSAP1-LDHA-Glycolysis-Lactate feedforward loop promotes Warburg effect and metastasis in pancreatic ductal adenocarcinoma. Cancer Lett 567:216285. https://doi.org/10.1016/j.canlet.2023.216285
35. Wang Q, Sun N, Meixner R, Le Gleut R, Kunzke T, Feuchtinger A, Wang J, Shen J, Kircher S, Dischinger U, Weigand I, Beuschlein F, Fassnacht M, Kroiss M, Walch A (2023) Metabolic heterogeneity in adrenocortical carcinoma impacts patient outcomes. JCI Insight. https://doi.org/10.1172/jci.insight.167007
36. Laubach K, Turan T, Mathew R, Wilsbacher J, Engelhardt J, Samayoa J (2023) Tumor-intrinsic metabolic reprogramming and how it drives resistance to anti-PD-1/PD-L1 treatment. Cancer Drug Resist 6:611–641. https://doi.org/10.20517/cdr.2023.60
37. Siqueira JM, Vega M, Pimentel GD (2023) Amino acids and cancer: potential for therapies? Curr Opin clin. Curr Opin Clin Nutr Metab Care https://doi.org/10.1097/MCO.0000000000000998. Nutr Metab Care
38. Castellano I, Gallo F, Durelli P, Monge T, Fadda M, Metovic J, Cassoni P, Borella F, Raucci C, Menischetti M, Beano A, Migliaretti G, Finocchiaro C (2023) Impact of caloric restriction in breast cancer patients treated with neoadjuvant chemotherapy: A prospective case control study. https://doi.org/10.3390/nu15214677
39. Yu Y, Wu J, Wu H, Wang Z, Wu S, Hong L, Xu B, Shao L (2023) A large-scale study integrating nutritional indicators and clinicopathological parameters to evaluate prognosis, follow-up, and postoperative chemotherapy decisions in rectal cancer patients. Support Care Cancer 31:686. https://doi.org/10.1007/s00520-023-08147-x
40. Huang HC, Wen XZ, Xue H, Chen RS, Ji JF, Xu L (2019) Phosphoglucose isomerase gene expression as a prognostic biomarker of gastric cancer. Chin J Cancer Res 31:771–784. https://doi.org/10.21147/j.issn.1000-9604.2019.05.07
41. Luo F, Li Y, Yuan F, Zuo J (2019) Hexokinase II promotes the Warburg effect by phosphorylating alpha subunit of pyruvate dehydrogenase. Chin J Cancer Res. https://doi.org/10.21147/j.issn.1000-9604.2019.03.14. 31:521–32
42. Xu J, Guo Y, Ning W, Wang X, Li S, Chen Y, Ma L, Qu Y, Song Y, Zhang H (2021) Comprehensive analyses of glucose metabolism in glioma reveal the glioma-Promoting effect of GALM. Front

Cell Dev Biol 9:717182. https://doi.org/10.3389/fcell.2021.717182
43. Mai WX, Gosa L, Daniels VW, Ta L, Tsang JE, Higgins B, Gilmore WB, Bayley NA, Harati MD, Lee JT, Yong WH, Kornblum HI, Bensinger SJ, Mischel PS, Rao PN, Clark PM, Cloughesy TF, Letai A, Nathanson DA (2017) Cytoplasmic p53 couples oncogene-driven glucose metabolism to apoptosis and is a therapeutic target in glioblastoma. Nat Med 23:1342–1351. https://doi.org/10.1038/nm.4418
44. Liu Y, Liu N, Zhou X, Zhao L, Wei W, Hu J, Luo Z (2023) Constructing a prognostic model for head and neck squamous cell carcinoma based on glucose metabolism related genes. Front Endocrinol (Lausanne) 14:1245629. https://doi.org/10.3389/fendo.2023.1245629
45. Miao X, Wang H, Fan C, Song Q, Ding R, Wu J, Hu H, Chen K, Ji P, Wen Q, Shi M, Ye B, Fu D, Xiang M (2023) Enhancing prognostic accuracy in head and neck squamous cell carcinoma chemotherapy via a lipid metabolism-related clustered polygenic model. Cancer Cell Int 23:164. https://doi.org/10.1186/s12935-023-03014-5
46. Zhou H, Wang F, Niu T (2022) Prediction of prognosis and immunotherapy response of amino acid metabolism genes in acute myeloid leukemia. Front Nutr 9:1056648. https://doi.org/10.3389/fnut.2022.1056648
47. Li X, Wenes M, Romero P, Huang SC, Fendt SM, Ho PC (2019) Navigating metabolic pathways to enhance antitumour immunity and immunotherapy. Nat Rev Clin Oncol 16:425–441. https://doi.org/10.1038/s41571-019-0203-7
48. Leone RD, Powell JD (2020) Metabolism of immune cells in cancer. Nat Rev Cancer. https://doi.org/10.1038/s41568-020-0273-y.
49. Sindhu S, Ahmad R (2023) Metabolic inflammation and cellular immunity. Cells https://doi.org/10.3390/cells12121615. Cells 12
50. Toes RE, Kast WM, Blom RJ, Bakker SC, Offringa R, Melief CJ (1996) Efficient tumor eradication by adoptively transferred cytotoxic T-cell clones in allogeneic hosts. Int J Cancer 66(5):686–691.
51. He W, Zhang H, Han F, Chen X, Lin R, Wang W, Qiu H, Zhuang Z, Liao Q, Zhang W, Cai Q, Cui Y, Jiang W, Wang H, Ke Z (2017) CD155T/TIGIT signaling regulates CD8(+) T-cell metabolism and promotes tumor progression in human gastric cancer. Cancer Res 77:6375–6388. https://doi.org/10.1158/0008-5472.CAN-17-0381
52. Byun JK, Park M, Lee S, Yun JW, Lee J, Kim JS, Cho SJ, Jeon HJ, Lee IK, Choi YK, Park KG (2020) Inhibition of glutamine utilization synergizes with immune checkpoint inhibitor to promote antitumor immunity. Mol Cell 80:592–606e8. https://doi.org/10.1016/j.molcel.2020.10.015
53. Ma G, Liang Y, Chen Y, Wang L, Li D, Liang Z, Wang X, Tian D, Yang X, Niu H (2020) Glutamine deprivation induces PD-L1 expression via activation of EGFR/ERK/c-Jun signaling in renal cancer. Mol Cancer Res 18:324–339. https://doi.org/10.1158/1541-7786.MCR-19-0517
54. Sharma MD, Baban B, Chandler P, Hou DY, Singh N, Yagita H, Azuma M, Blazar BR, Mellor AL, Munn DH (2007) Plasmacytoid dendritic cells from mouse tumor-draining lymph nodes directly activate mature Tregs via indoleamine 2,3-dioxygenase. J Clin Invest 117:2570–2582. https://doi.org/10.1172/JCI31911
55. Yang B, Wang X, Ren X (2012) Amino acid metabolism related to immune tolerance by MDSCs. Int Rev Immunol 31:177–183. https://doi.org/10.3109/08830185.2012.679989
56. Jiang F, Luo F, Zeng N, Mao Y, Tang X, Wang J, Hu Y, Wu C (2022) Characterization of fatty acid Metabolism-Related genes landscape for predicting prognosis and aiding immunotherapy in glioma patients. Front Immunol 13:902143. https://doi.org/10.3389/fimmu.2022.902143
57. Ferreri AJ, Montalban C (2007) Primary diffuse large B-cell lymphoma of the stomach. Crit Rev Oncol Hematol 63:65–71. https://doi.org/10.1016/j.critrevonc.2007.01.003
58. Ruskone-Fourmestraux A, Dragosics B, Morgner A, Wotherspoon A, De Jong D (2003) Paris staging system for primary Gastrointestinal lymphomas. Gut 52:912–913. https://doi.org/10.1136/gut.52.6.912
59. Vasiliou V, Thompson DC, Smith C, Fujita M, Chen Y (2013) Aldehyde dehydrogenases: from eye crystallins to metabolic disease and cancer stem cells. Chem Biol Interact 202:2–10. https://doi.org/10.1016/j.cbi.2012.10.026
60. Muzio G, Maggiora M, Paiuzzi E, Oraldi M, Canuto RA (2012) Aldehyde dehydrogenases and cell proliferation. Free Radic Biol Med. https://doi.org/10.1016/j.freeradbiomed.2011.11.033. 52:735–46
61. Kuang Y, Feng J, Jiang Y, Jin Q, Wang Q, Zhang C, He Y (2023) Prognostic and immunological role of acetaldehyde dehydrogenase 1B1 in human tumors: A pan-cancer analysis. Int J Immunopathol Pharmacol 37:3946320231206966. https://doi.org/10.1177/03946320231206966
62. Singh S, Chen Y, Matsumoto A, Orlicky DJ, Dong H, Thompson DC, Vasiliou V (2015) ALDH1B1 links alcohol consumption and diabetes. Biochem Biophys Res Commun 463:768–773. https://doi.org/10.1016/j.bbrc.2015.06.011
63. Tsochantaridis I, Roupas A, Voulgaridou GP, Giatromanolaki A, Koukourakis MI, Panayiotidis MI, Pappa A (2021) Aldehyde dehydrogenase 1B1 is associated with altered cell morphology, proliferation, migration and chemosensitivity in human colorectal adenocarcinoma cells. Biomedicines. https://doi.org/10.3390/biomedicines9010044
64. Mameishvili E, Serafimidis I, Iwaszkiewicz S, Lesche M, Reinhardt S, Bolicke N, Buttner M, Stellas D, Papadimitropoulou A, Szabolcs M, Anastassiadis K, Dahl A, Theis F, Efstratiadis A, Gavalas A (2019) Aldh1b1 expression defines progenitor cells in the adult pancreas and is required for Kras-induced pancreatic cancer. Proc Natl Acad Sci U S A 116:20679–20688. https://doi.org/10.1073/pnas.1901075116
65. Wang X, Li C, Yao W, Tian Z, Liu Z, Ge H (2020) MicroRNA-761 suppresses tumor progression in osteosarcoma via negatively regulating ALDH1B1. Life Sci 262:118544. https://doi.org/10.1016/j.lfs.2020.118544
66. Wang H, Li Y, Zhou D, Li X, Jia S, Qi S, Huang J (2021) Aldehyde dehydrogenase 1B1 is a potential marker of colorectal tumors. Histol Histopathol 36:183–194. https://doi.org/10.14670/HH-18-304
67. Feng Z, Hom ME, Bearrood TE, Rosenthal ZC, Fernandez D, Ondrus AE, Gu Y, McCormick AK, Tomaske MG, Marshall CR, Kline T, Chen CH, Mochly-Rosen D, Kuo CJ, Chen JK (2022) Targeting colorectal cancer with small-molecule inhibitors of ALDH1B1. Nat Chem Biol 18:1065–1075. https://doi.org/10.1038/s41589-022-01048-w